REGULATION OF METABOLIC OSCILLATIONS AT SINGLE ISLETS OF LANGERHANS AS STUDIED BY AMPEROMETRIC MEASUREMENTS OF RESPIRATION AND GLUCOSE METABOLISM

By

LISA MARIE KAURI

A DISSERTATION PRESENTED TO THE GRADUATE SCHOOL
OF THE UNIVERSITY OF FLORIDA IN PARTIAL FULFILLMENT
OF THE REQUIREMENTS FOR THE DEGREE OF
DOCTOR OF PHILOSOPHY

UNIVERSITY OF FLORIDA

2002

To my family, for their continued support and love.

ACKNOWLEDGMENTS

During my years at graduate school many people have been there to advise, help and encourage me along the way. For sharing the experience of graduate school I would like to thank all the past and present members of the Kennedy group, especially Charina and Craig for teaching me what analytical chemistry is all about, Sung and Gabriella for collaborative efforts and Danielle B, Jacinth, Rebecca, Holly, Jonnie, Jennifer P and Jonathan for making life in the lab more enjoyable. I would like to thank Dave, Damian, Gunnar, Elizabeth and Dean for dragging me out of lab for either exercise or parties, both of which made life in Florida more enjoyable. I would also like to thank Dr. Robert T. Kennedy for his guidance, assistance and support throughout my graduate career.

For encouragement and help throughout my journey before and during graduate school, I would like to thank my family and friends. My immediate family including Tiiu, Tiit, Piia and Dave have always been there to applaud my accomplishments and support me when things became difficult. I took inspiration from Hans, Reet and Ivi, all accomplished in their own fields of study and who were always there to encourage and assist me. I would like to thank my dear friends Laurelle, Becky, Sylvia, Danielle C, Taimi and Patrick for reminding me that outside of graduate school life continues and I need to join the outside world once again.

TABLE OF CONTENTS

Page

ACKNOWLEDGMENTS iii

LIST OF ABBREVIATIONS vi

CHAPTERS

1 INTRODUCTION 1

Beta-cells and Islets of Langerhans 2
Detection of Insulin 4
Glucose Induced Insulin Secretion 7
Insulin Oscillations 10
Proposed Mechanisms of Insulin Pulsatility 11
Oscillations in Oxygen Consumption 13
Oscillations in Glucose Consumption 15
Oscillations in Other Metabolic Parameters 15
Dissertation Overview 17

2 EFFECT OF SUBSTRATE USED ON METABOLIC OSCILLATIONS 21

Introduction 21
Experimental 24
Results and Discussion 25
Glyceraldehyde and Metabolic Oscillations 26
Ketoisocaproate and Metabolic Oscillations 28
Pyruvate and Methyl Pyruvate Metabolism 31
Slow Versus Fast Oscillations 33
Conclusions 35

3 INTRACELLULAR CALICUM MODIFIERS AND METABOLIC OSCILLATIONS 38

Introduction 38
Experimental 40
Results and Discussion 42
Extracellular Calcium 42
Pulsing K+ 43
Diazoxide 45
Diazoxide and Pulsing K^+ 48
Mitochondrial Ca^{2+} Exchange 50

Mitochondrial Na^+-Ca^{2+} Exchanger 50
Mitochondrial Ca^{2+} Influx 51
Conclusions 53

4 GLUCOSE TRANSPORT INTO ISLETS OF LANGERHANS 55

Introduction 55
Experimental 57
Results and Discussion 58
Islet Size 58
Glucokinase Inhibition 60
Glucose Incubation Concentration 60
Extracellular Ca^{2+} 64
Conclusions 65

5 OTHER METABOLIC FACTORS 66

Introduction 66
Experimental 68
Results 70
Amino Acid Rich Media 70
IRS-1 Knock-Out Islets 73
Glucose Incubation Concentration 74
Conclusions 77

6 INSULIN ELECTRODE 78

Introduction 78
Experimental 80
Results and Discussion 82
Components of Plating Solution 82
Electrochemical Plating Procedure 84
Conclusions 90

7 SUMMARY AND FUTURE DIRECTIONS 92

Summary 92
Future Directions 94

APPENDIX A : OXYGEN AND GLUCOSE SENSORS 97

APPENDIX B : MURINE ISLET ISOLATION 102

APPENDIX C : AMPEROMETRIC SETUP 105

LIST OF REFERENCES 107

BIOGRAPHICAL SKETCH 118

LIST OF ABBREVIATIONS

$[ATP]_c$	cytosolic ATP concentration
$[Ca^{2+}]_c$	cytosolic Ca^{2+} concentration
$[Ca^{2+}]_i$	intracellular Ca^{2+} concentration
$[Ca^{2+}]_m$	mitochondrial Ca^{2+} concentration
CE	capillary electrophoresis
CGP 37157	7-chloro-5-(2-chlorophenyl)-1,5-dihydro-4,1-benzothiazepin-2(3*H*)-one
DMEM	Dublecco's Modified Eagle Medium
FCCP	carbonyl cyanide 4-(trifluoromethoxy)phenylhydrazone
F16P	fructose-1,6-bisphosphate
GA	gluceraldehyde
GK	glucokinase
G1P	glyceraldehyde-1-phosphate
G3P	glyceraldehyde-3-phosphate
GPD	glyceraldehyde phosphate dehydrogenase
GSIS	glucose stimulated insulin secretion
HEPES	N-2-hydroxyethylpiperazine-N'-2-ethane sulfonic acid
HK	hexokinase
5HT	5-hydroxytryptamine

IRS	insulin receptor substrate
K_{ATP}	ATP sensitive K^+ (channel)
KIC	alpha-ketoisocaproate
K_m	Michaelis-Menten constant
KRB	Krebs-Ringer buffer
LC	liquid chromatography
LIF	laser induced fluorescence
LOD	limit of detection
MALDI-MS	matrix assisted laser desorption ion mass spectrometry
MLOD	mass limit of detection
MPDA	metaphenylene diamine
2-NBDG	2-[N-(7-nitrobenz-2-oxa-1,3-diazol-4-yl)amino]2-deoxy-D-glucose
PFK	phosphofructokinase
PK	pyruvate kinase
RHPA	reverse hemolytic plaque assay
RIA	radioimmunoassay
SSCE	saturated sodium calomel electrode
t_r	retention time
USN/MC-ES-MS	ultrasonic nebulization/multiple channel electrospray ionization mass spectrometry
V_{max}	maximum velocity of an enzymatic reaction

Abstract of Dissertation Presented to the Graduate School
of the University of Florida in Partial Fulfillment of the
Requirements for the Degree of Doctor of Philosophy

REGULATION OF METABOLIC OSCILLATIONS AT SINGLE ISLETS OF LANGERHANS AS STUDIED BY AMPEROMETRIC MEASUREMENTS OF RESPIRATION AND GLUCOSE METABOLISM

By

Lisa Marie Kauri

May 2002

Chairman: Robert T Kennedy
Major Department: Chemistry

Type 2 diabetes mellitus results from the inability to maintain glucose homeostasis through insulin production, secretion or utilization. Glucose stimulated insulin secretion occurs through the following mechanism. With increasing glucose levels, beta cells from pancreatic islets of Langerhans release insulin. As glucose is metabolized in beta cells, oxygen is consumed and the intracellular calcium concentration ($[Ca^{2+}]_i$) increases, initiating insulin secretion from the beta cell. Serum insulin and glucose levels oscillate with a period of 4 to 14 minutes. These oscillations are beneficial since with oscillations a lower amount of insulin is required to activate receptors than with a constant level. In with type 2 diabetes oscillations in serum insulin levels are lost.

In vitro, single islets of Langerhans display oscillations in insulin secretion and $[Ca^{2+}]_i$. Using sensors developed in our laboratory, oscillations in glucose and oxygen levels have been monitored at single islets of Langerhans exposed to stimulatory glucose

levels. Using these sensors, it has been shown that oscillations in glucose and oxygen levels were dependent on the presence of extracellular Ca^{2+} and were abolished when $[Ca^{2+}]_i$ was held constant. Changes induced in $[Ca^{2+}]_i$ through control of K_{ATP} channels caused changes in both oxygen and glucose consumption; however, no spontaneous oscillations were observed in the absence of metabolic substrates. In addition only stimulatory levels of glucose induced slow oscillations (> 1 min.) in oxygen levels. However, glyceraldehyde, a glycolytic substrate, can induce fast oscillations (10-35 s.), while pyruvate, the end product of glycolysis, is unable to induce any oscillations in oxygen levels. Thus, either a glycolytic enzyme or a signaling molecule produced during the early steps of glycolysis is required to produce slow oscillations in glucose and oxygen levels. Under conditions that resemble hypoglycemia or hyperglycemia, isolated islets displayed no slow oscillations in glucose levels. Lastly using glucose sensors the glucose equilibration within an islet following a change in extra-islet glucose level was shown to be controlled by glucose transport into and consumption by peripheral beta-cells.

CHAPTER 1
INTRODUCTION

Insulin, secreted by pancreatic beta-cells, promotes glucose uptake and metabolism by liver, muscle and adipose tissue. Inadequate insulin secretion by beta-cells for peripheral tissue activation results in diabetes. Diabetes is a group of diseases that result in the inability of the body to maintain blood glucose homeostasis. In America alone, 17,000,000 people suffer from diabetes. The majority of diagnosed diabetics suffer from type 2 diabetes, a condition where the beta-cells secrete inadequate amounts of insulin.

Type 1 diabetes is characterized by an autoimmune response, often occurring during early childhood, resulting in the destruction of beta-cells, leaving the afflicted individual dependent on insulin treatment. Research into treatments of type 1 diabetes includes investigations of insulin delivery, beta-cell transplantation, as well as generation of new beta-cells from stem cells.

In type 2 diabetes, beta-cells are not destroyed but secrete insulin at a reduced rate, which, when combined with the reduction of insulin receptor sensitivity in target tissue, results in a decrease in glucose uptake. In healthy individuals a glucose challenge promotes a two phase response in insulin secretion. Immediately following an increase in plasma glucose levels, a large increase in plasma insulin level occurs, called the first phase insulin release. Type 2 diabetics often lose the first phase of insulin release observed in plasma. Isolated islets from healthy individuals, but not those isolated from type 2 diabetics, exhibit a distinct first phase insulin secretion in response to a glucose

challenge [Del02]. The first phase of insulin secretion is followed by a decrease to a lower, yet elevated, plasma insulin level called the second phase. Oscillations in plasma insulin level can be observed during the second phase. Type 2 diabetics display a reduced level of insulin release during the second phase and display erratic or non-existent pulsatility of serum levels. Research into type 2 diabetes has centered on understanding why some individuals are unable to maintain glucose homeostasis. Both the insulin secreting cells and peripheral tissue activated by insulin have been studied over the years, with emphasis on the amount and mechanism of normal insulin secretion and the body's response to it.

Beta-cells and Islets of Langerhans

Islets of Langerhans are found within the endocrine tissue of the pancreas. An estimated 13,500 and 890,000 islets exist per rat and human pancreas, respectively, and they vary in size from 50 to 400 μm in diameter [Nor97]. Figure 1-1 shows a picture of a murine islet 150 μm diameter. Islets are well-organized micro-organs, containing about 3,000 cells [Orc88]. Blood enters the islets through arterioles, which differentiates into capillaries in the islet, this allows for rapid transfer of blood glucose levels into the islet and secretion of hormones into the blood stream [Nor97].

Insulin secreting beta-cells are the most abundant cells within the islet. Depending on species beta-cells make up 70-90% of the islet. At least three other types of cells are also found in islets: alpha, gamma and PP cells, which respectively secrete glucagon, somatostatin and pancreatic polypeptide (PP) [Orc88]. Insulin induces cellular glucose uptake from the blood stream, whereas, glucagon induces catabolic reactions

Figure 1-1 Islet of Langerhans. Islet was 150 μm in diameter.

which lead to glucose release; thus, counteracting insulin [Nor97]. PP regulates the release of pancreatic digestive enzymes and somatostatin inhibits secretion of insulin, glucagon and PP [Orc88]. Thus, the islet cells are capable of regulating blood glucose levels. After a meal blood glucose levels increase and islets respond through insulin secretion from beta-cells. In response to the insulin secreted target tissue, such as liver, muscle and adipose tissue, increase glucose uptake, reducing blood glucose levels [Nor97]. During fasting, glucose levels decrease reducing insulin secretion and increasing glucagon release, which activates glucose stored within the body.

Beta-cells secrete insulin in discrete packets contained in vesicles in response to a stimulation, such as glucose. In vesicles, insulin exists in a hexamer complex with two Zn^{2+} ions [Asp97, Blu72, Emd80, Gol84]. The hexamer complex is insoluble at pH below 7 [Blu72, Emd80, Epa85, Tan54]; therefore, the insulin complex is solid within the vesicle as the intra-vesicle pH is maintained at or below pH 6 [Hut82, Orc85]. During exocytosis, the vesicles fuse with the outer cellular membrane and release their contents into the extracellular environment. Since extracellular pH is maintained above pH 7, the insulin-Zn^{2+} complex dissociates, and free insulin leaves the beta-cell.

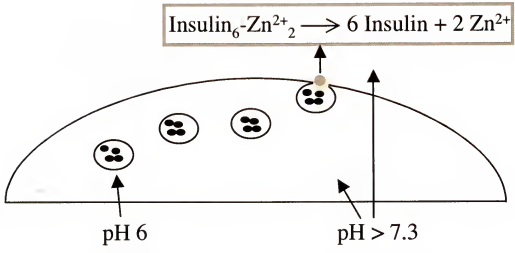

Figure 1-2 Insulin release from beta-cell. Within the secretory vesicle insulin is in a hexameric complex with two Zn^{2+} ions, after vesicle fusion the vesicle pH increases to above 7.3, allowing for dissociation of the complex.

Detection of Insulin

Monitoring insulin secretion in response to stimuli, such as elevated glucose levels, can assist the investigations into the signal coupling for normal insulin secretion. Various analytical techniques such as immunoassays [Yal60], spectrochemical methods [Dem85, Sch60], and amperometry [Cox84, Ken93] have been developed for insulin detection. Table 1-1 gives a summary of detection methods with limits of detection (LOD). However, it should be noted that techniques, such as microelectrodes, which monitor single exocytosis events of insulin secretion have mass limits of detection (MLOD) less than 1 amol. The techniques utilized for insulin detection can be separated into three categories; secretion measurements, tissue samples or blood glucose levels, and techniques which have good potential for insulin detection, but have not been applied to biological samples.

Insulin detection in tissue samples dates back to 1960, when pseudoisocyanins were reacted with insulin to produce a metachromasia (product having different color

than reactant), which was detected through absorbance measurements. [Sch60]. This method had been applied to tissue samples where the beta-cell cytoplasmic granules were preferentially stained. This method had also been applied to solutions containing insulin from samples obtained during insulin manufacture.

Table 1-1 Summary of methods used for insulin detection.

Detection Method	Reference	LOD From Reference	LOD (nM)
Silver Stain Protein Assay	Kry85	10 ng/100 μL	16
Chemiluminescent Immunoassay	Cao01	5 pM	0.005
LIF and CE Competitive Immunoassay	Tao96	0.3 nM	0.3
Microcolumn LC and Competitive Immunoassay	She97	10 fmol/500 μL	0.020
Fluorescent Derivatized Insulin and Competitive Chromatograph	Liu01	26 pg /5 μL	0.035
Micellar Electrokinetic Capillary Chromatography	Den02	0.01 mg/mL	~1500
Modified Electrode	Cox89	2 ng/7.5 μL	40
Modified Microelectrode	Ken93	0.5 μM	500
Modified Microelectrode	Gor97	23 nM	23
MALDI-MS[a]	Arm01	100 fmol/μL	100
USN/MC-ES-MS[b]	Shi01	$< 10^{-6}$ M	1000

a MALDI-MS = matrix assisted laser desorption ion mass spectrometry.
b USN/MC-ES-MS=ultrasonic nebulization/multiple channel electrospray ionization mass spectrometry.

The first group of techniques to become prevalent for detection of insulin in serum samples, were based on immunoassays specific for insulin. Insulin levels have been monitored in serum and plasma utilizing radio-immunoassays (RIA) [Bel71, Ber59, Sta74, Tal60]. Increased specificity of RIA was obtained with an enzyme-linked two-site

immunoassay [And93]. Chemiluminescent enzyme immunoassays have also been developed for monitoring serum samples [But01, Cao01]. Utilizing RIA for insulin detection has been extended to monitor insulin secretion from groups of islets or clonal beta-cells [Aiz00, Ble96, Kan92, Opa92]. However, samples for RIA analysis are obtained as aliquot samples of run buffer from groups of islets or cells, resulting in poor temporal resolution (>6 s) [Aiz00].

Spectrophotometric detection methods have been developed to measure insulin secretion from tissues. Employing Coomassie blue and/or silver staining with electrophoresis in sodium dodecyl sulfate-polyacrylamide gels has allowed for separation and detection of insulin secreted from tissue samples [Dem85, Kry85, Kry87, Mor81].

Fluorescent derivatization of insulin has allowed for secretion measurements from single islets utilizing competitive immunoassays. Insulin secretion from single rat islets has been monitored through coupling microcolumn liquid chromatography [Sch95, She97] or capillary electrophoresis [Tao96] with fluorescently labeled insulin during competitive immunoassay [She97]. Three possible labeling sites exist on insulin; however, most fluorescent derivatization reactions indiscriminately label insulin, resulting in the need of a clean-up step for the fluorescently labeled insulin prior to experiments. It has been shown that insulin can be triply labeled while retaining its immunoaffinity for the antibody and can be applied to competitive chromatographic immunoassays [Liu01]. The triply labeled insulin increases sensitivity of competitive chromatographic methods; thus, this method has high potential for monitoring insulin secretion from islets, and possibly sensitive enough for single beta-cells.

Insulin secretion from single beta-cells have been monitored using reverse hemolytic plaque assay (RHPA) [Chi87, Hir88, Hir95]. In this technique beta-cells are incubated with red blood cells conjugated with protein A, then the cells are incubated with an insulin antiserum. Next a complement is added which lyses the red blood cells displaying insulin anti-insulin complexes bound to the protein A. Thus, the insulin released during insulin antiserum incubation can be visualized by the presence of a haemolytic plaque surrounding the secretory cells.

Amperometry at microelectrodes has been successfully utilized to monitor insulin secretion from single beta-cells. Modified microelectrodes capable of detecting insulin were developed [Che01, Cox89, Gor97] and applied to detection of insulin secretion from single canine and human beta-cells [Hua95, Ken93]. However, these electrodes degrade quickly at biological pH and were not capable of monitoring insulin secretion from rodent beta-cells. As an alternative, beta-cells can be incubated with 5-hydroxytryptamine (5HT), which accumulates in the insulin-containing secretory vesicles and is co-secreted with insulin. 5HT can be then be detected at bare carbon fiber microelectrodes and used as an indirect measure of the insulin secretion. Utilizing this technique, insulin secretion has been monitored at single beta-cells of various species [Asp97, Bar96, Par97, Zho96], including canine, murine and porcine.

A method has recently been developed, utilizing the fact that Zn^{2+} is co-secreted with insulin. Using a Zn^{2+} fluorescence dye, a technique has been developed which monitors the Zn^{2+} co-released with insulin with a confocal microscope [Qia00]. This technique has been successfully applied to single beta-cells, groups of beta-cells and single islets.

Recently, techniques utilizing mass spectrometry have been developed. MALDI-MS [Arm01] and USN/MC-ES-MS [Shi01] have enabled insulin detection with low MLODs. Application of MS to real life samples, such as serum samples or secretions from beta-cells, could improve insulin detection from small samples.

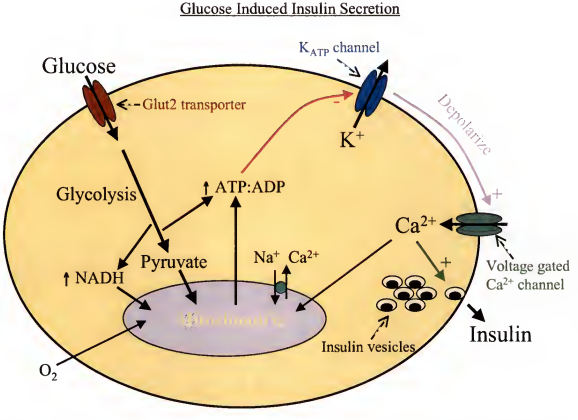

Figure 1-3 Summary of beta-cell signal coupling involved in glucose induced insulin secretion. Signals which activate or inhibit specific cellular activities are denoted by + or – respectively.

Glucose is the primary insulin secretagogue *in vivo*. The consensus model for the mechanism of glucose stimulated insulin release (GSIS) is illustrated in Figure 1-3 [Dee00, Hen00, Kom97, Mat96, New95]. Glucose is transported into beta-cells via glucose transporters. About 80% of glucose is transported into the beta-cell via the glucose transporter Glut2, while the remaining 20% is transported by Glut1 [Yas92,

Yos96]. Glut2, unlike Glut1, is reversible, allowing glucose to be transported into and out of the cell. Glut2 has a relatively high K_m for glucose (17-20 mM), insuring that as glucose levels increase there is a linear increase in glucose transport into the beta-cell [Gou97]. Glut1 has a much lower K_m (1.6 mM) than Glut2 and can only transport glucose into beta-cells, allowing glucose to be transported into the beta-cell during times of low extracellular glucose levels preventing cell starvation [Gou97].

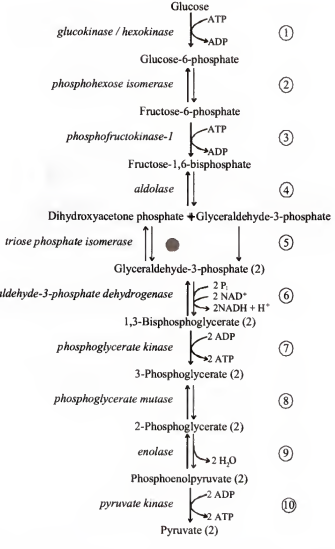

Figure 1-3 The ten steps of glycolysis, enzymes written in italics.

After transport into the beta-cell, glucose is metabolized by glycolysis, which is the only method of glucose metabolism in beta-cells. Glycolysis consists of 10 enzymatically driven reactions producing increases in the ATP:ADP ratio, NADH and pyruvate levels (Fig 1-3). The first enzyme in glycolysis is glucokinase (GK), also called hexokinase IV, is often referred to as the "glucose sensor" of the beta-cell, since it is rate limiting for glucose consumption and the K_m for glucose (5-17 mM) [Bed86, Hel74, Lia90, Meg84, Tru81] is similar to the glucose concentration required for half-maximal response in insulin secretion. Pyruvate enters the mitochondria and is metabolized through the citric acid cycle. The reducing equivalents from NADH enter the mitochondria through either the malate-aspartate shuttle or the glycerol-3-phosphate shuttle. The energy produced during the citric acid cycle and from NADH is transferred to ATP through oxidative phosphorylation (consuming oxygen in the process) increasing the ATP:ADP ratio [Duk94, Sch97, Eto99a, Eto99b]. The increase in ATP/ADP ratio closes ATP sensitive potassium (K_{ATP}) channels, depolarizing the beta-cell [Coo84, Ash84, Koh98] and opening voltage gated calcium channels [Ror88]. The resulting increase in intracellular Ca^{2+} level ($[Ca^{2+}]_i$) initiates insulin secretion by exocytosis.

Insulin Oscillations

Serum insulin and glucose levels oscillate with a period of 4 to 14 minutes in healthy individuals [Goo77, Hol02, Lan79, Por97], but individuals with type 2 diabetes and their close relatives often display erratic or non-existent pulsatility of serum insulin levels [Ora88, Mat83]. The importance of pulsatile blood glucose levels has been demonstrated by the greater effect of pulsatile versus steady state insulin infusions *in vivo* on glucose uptake [Koo96, Mat83, Pao87, Pao88]. Recently it was shown that 75% of insulin release in humans arises from pulses in insulin release [Por97].

Since the discovery of serum insulin pulsatility, many studies have tried to elucidate the chemical mechanisms underlying oscillations in insulin secretion. Islets of Langerhans also display pulsatility in insulin secretion, although with a faster period (0.5 to 3 min) [Bar96, Ber93, Ber94, Gil93], which shows that insulin pulsatility is inherent in islets. Simultaneous measurements have shown $[Ca^{2+}]_i$ and insulin secretion oscillate parallel to each other [Gil93].

Proposed Mechanisms of Insulin Pulsatility

The exact mechanism underlying insulin pulsatility has yet to be elucidated, but two models consistent with GSIS have been proposed. The first model proposes that inherent oscillations in glucose metabolism are the basis of oscillations in beta-cells [Tor97]. Glycolysis has been shown to oscillate in several systems [Hes71, Job67, Job68, Tor88, Tor91], and these oscillations have been suggested to serve as a pacemaker, entraining other cellular processes in the beta-cell. Four glycolytic enzymes have feedback regulation appropriate for oscillation generation, including GK, phosphofructokinase (PFK), glyceraldehyde phosphate dehydrogenase (GPD), and pyruvate kinase (PK) [Mac97, Ris97, Ris99]. PFK and GPD are active during low ATP:ADP and NADH:NAD ratios, respectively; however, high levels of ATP also inhibit PFK. PFK and PK are both activated by fructose-1,6-bisphosphate (F16P), the product of PFK. GK is inhibited by acylCoA [Mac97] and during incubation in high glucose levels an increase in the V_{max} of GK is observed [Pur93]. Although all these enzymes can potentially generate oscillations in beta-cells, GK and PFK have more complex feedback systems; therefore, GK and PFK are believed to have a larger influence on glucose usage by beta-cells than GPD or PK [Mat90, Tor97]. The activity of PFK in cell-free extracts from skeletal muscle has been shown to oscillate, and the

addition of inhibitors and activators of PFK activity modulate these bursts of activity [Tor88, Tor91]. Thus, it is believed that *in vivo* the PFK driven reaction oscillates in response to substrate and product concentrations, and that it entrains other cellular processes into this oscillatory activity [Tor97]. Clinical evidence has shown that defects in both GK and PFK are linked to derangement in pulsatility of insulin secretion and predisposition to type 2 diabetes [Fro92, Fro93, Hat92, Mah99, Per92, Ris99, Vel97].

The second model consistent with GSIS proposed for oscillatory insulin secretion is based on the observation that K_{ATP} channel conductance is involved in Ca^{2+} regulated oscillations [Hen90, Rol02, Gil02]. In this model, glucose enters the beta-cell and is metabolized, increasing the ATP:ADP ratio, closing K_{ATP} channels, and depolarizing the cell membrane. The depolarization opens voltage gated Ca^{2+} channels increasing $[Ca^{2+}]_i$, triggering exocytosis as well as ATP consumption, decreasing ATP:ADP ratio. The decrease in ATP:ADP reopens K_{ATP} channels decreasing Ca^{2+} entry; thus, decreasing $[Ca^{2+}]_i$ [Hen90]. The decrease in $[Ca^{2+}]_i$ decreases ATP consumption, increasing ATP:ADP ratio; thus, starting another cycle and producing oscillations. In beta-cells, oscillations in cytosolic Ca^{2+} concentration ($[Ca^{2+}]_c$) imposed by repetitive membrane depolarizations using 30 mM K^+ in the presence of diazoxide were accompanied by oscillations in insulin secretion. When the $[Ca^{2+}]_c$ was later held constant by long term 30 mM K^+ induced depolarization, the insulin secretion stayed constant [Jon98]. To test the effect of glucose metabolism on insulin secretion while $[Ca^{2+}]_c$ was held constant, glucose levels were pulsed in the presence of constant 30 mM K^+ and diazoxide. $[Ca^{2+}]_c$ remained elevated and constant, while pulses were observed in NAD(P)H and insulin levels. However, the insulin pulses were greatly reduced by about 100 fold as compared

to pulses generated by pulsing K^+ levels [Rav99]. From these experiments $[Ca^{2+}]_c$ was concluded to be the main driver of oscillatory insulin secretion [Gil02].

Oscillations in Oxygen Consumption

Recently there has been mounting evidence that not only insulin secretion and $[Ca^{2+}]_i$ but also metabolic factors, such as oxygen and glucose levels, oscillate in islets. Monitoring oxygen consumption at a group of islets revealed that similar oscillatory patterns were seen in oxygen consumption as those previously observed in $[Ca^{2+}]_i$ [Lon91]. However, the changes in oxygen level observed in this study were noise dominated; thus, to investigate oscillations in respiration at single islets with good sensitivity were required. Figure 1-5 shows oxygen level at an islet in response to increasing glucose level from 3 to 10 mM monitored at oxygen sensors developed in our laboratory [Jun99a, Jun99b]. For these measurements oxygen sensors were implanted into islets, as shown in Figure 1-6; thus, the extra-cellular intra-islet oxygen levels were monitored. Therefore, a decrease in oxygen level represents increased oxygen consumption by the beta-cells within the islet.

Oxygen consumption was shown to oscillate in single islets of Langerhans in similar patterns to those previously observed in $[Ca^{2+}]_i$ [Jun99a, Jun99b, Ort00]. These oscillations manifest themselves as fast oscillations with a period of 17 +/- 3 s (n=10), slow oscillations with a period of 197 +/- 10 s (n=11), or slow oscillations with fast oscillations superimposed (Chapter 2). It was also shown that oscillations in oxygen consumption were dependent on extracellular Ca^{2+} levels and that oxygen consumption increased in response to increasing glucose levels [Jun99a]. To verify that oxygen consumption was indeed being monitored, rotenone, an inhibitor of mitochondrial respiration, was applied to an islet in the presence of stimulatory levels of glucose. This

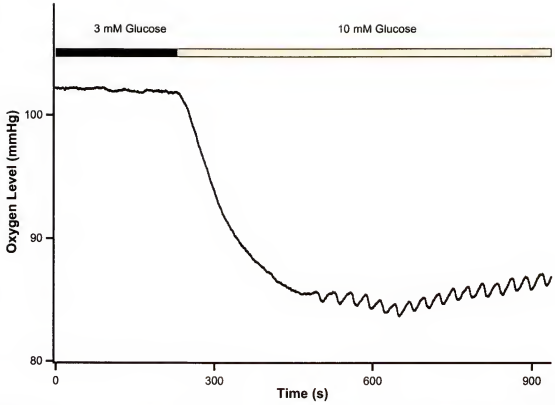

Figure 1-5 Oxygen consumption observed at an islet in response to a glucose challenge. Oxygen sensor was implanted to 70 μm into the islet, while glucose levels were increased from 3 to 10 mM.

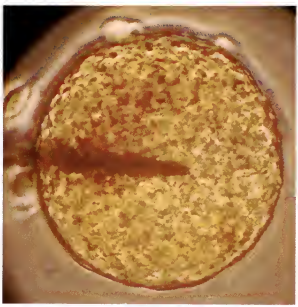

Figure 1-6 Oxygen sensor implanted into an islet of Langerhans (150 μm in diameter).

resulted in a decrease in oxygen consumption and an abolishment of oscillations [Jun99b]. During the initial response of an islet to a glucose challenge, changes in oxygen consumption precede changes in $[Ca^{2+}]_i$. However, when the cellular activity of an islet has settled into oscillatory activity, changes in $[Ca^{2+}]_i$ precede that of oxygen consumption, with oxygen consumption increasing with increases in $[Ca^{2+}]_i$ [Jun00], supporting the idea that Ca^{2+} plays an important role in causing metabolic oscillations.

Oscillations in Glucose Consumption

To investigate further metabolic oscillations at an islet, a sensor capable of monitoring glucose consumption at an islet was developed in our laboratory [Jun00]. These were the first sensors capable of monitoring changes in glucose levels at single islets. Figure 1-7 shows the effect of increasing extra-islet glucose level while monitoring glucose consumption inside an islet. It was shown that glucose consumption oscillates parallel, but lags $[Ca^{2+}]_i$ oscillations by 5 s. Similar patterns of oscillations were observed in glucose consumption as that with $[Ca^{2+}]_i$ and oxygen consumption [Jun00]. Application of mannoheptulose, a competitive inhibitor of glucokinase, resulted in abolishment of oscillations [Jun00] illustrating that the oscillations in glucose level were the result of oscillating glucose consumption.

Oscillations in Other Metabolic Parameters

ATP:ADP ratio is an important signal transducer within the beta-cell because an increase in this ratio is believed to cause the characteristic plasma membrane depolarization observed in beta cells exposed to high levels of glucose. Observations of oscillations in K_{ATP} conductance in beta-cells suggested oscillations in ATP:ADP levels [Lar96].

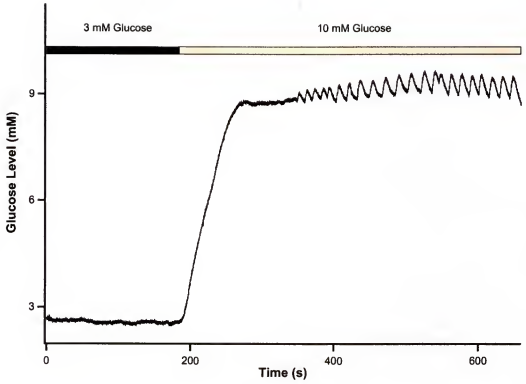

Figure 1-7 Glucose level observed at an islet in response to a glucose challenge. An increase in glucose level is equivalent to a decrease in glucose consumption. Glucose sensor was implanted to 70 μm into the islet, while glucose levels were increased from 3 to 10 mM.

However, only recently with the aid of recombinant luciferase expressed within islet beta cells could oscillations in cytosolic ATP concentration ($[ATP]_c$) be observed [Ain02]. It was revealed that increasing $[Ca^{2+}]_i$ using 30 mM K^+ increased $[ATP]_c$ and that glucose induced $[ATP]_c$ increase was reduced in the absence of Ca^{2+} [Ain02].

In response to stimulatory levels of glucose, NAD(P)H levels have been shown to oscillate in single beta-cells and islets [Gil92, Pra90, Pra94]. NAD(P)H levels were also increased by K^+ or glucose induced increases in $[Ca^{2+}]_i$ [Gil92, Pra90, Pra94]. Mitochondrial membrane potential has also been shown to oscillate in beta-cells [Kri00]. The oscillations in mitochondrial membrane potential were shown to occur in parallel to $[Ca^{2+}]_i$, with the depolarization actually happening in response to a change in cytosolic

Ca^{2+} concentration ($[Ca^{2+}]_c$) and not glucose [Kri00].

Dissertation Overview

Insulin secretion and $[Ca^{2+}]_i$ have been shown to oscillate in islets. Recently, evidence supporting the occurrence of metabolic oscillations has increased as observed by monitoring ATP, NADH, mitochondrial membrane potential, glucose consumption and oxygen consumption. However, the chemical mechanism underlying these oscillations is unknown. In this dissertation, glucose and oxygen sensitive sensors developed in our laboratory have been utilized to investigate the chemical mechanisms underlying oscillations in beta-cells.

One model consistent with GSIS proposes inherent oscillations in glucose metabolism as the basis oscillations in beta-cells. In Chapter 2 we investigate this theory by monitoring oxygen consumption at islets in response to different metabolic fuels. The metabolic fuels utilized in this study included two substrates of glycolysis, glucose and glyceraldehyde (GA), the end product of glycolysis, pyruvate, and a substrate of the citric acid cycle, alpha-ketoisocaproate (KIC). It was found that islets exhibited slow oscillations in oxygen consumption only in the presence of stimulatory levels of glucose. GA, but not pyruvate, could induce fast oscillations. KIC was able to induce small pulses in oxygen consumption; however, these pulses in oxygen consumption had much smaller magnitude than glucose or GA induced oxygen oscillations, and were irregular. These data suggest that slow and fast oscillations are generated by different mechanisms.

Another model consistent with GSIS proposes changes in $[Ca^{2+}]_i$ as the basis of oscillations. Previously, we have shown that changes in $[Ca^{2+}]_i$ tend to precede changes in glucose and oxygen consumption, during oscillations. Chapter 3 further investigates the effect of $[Ca^{2+}]_i$ on metabolic oscillations. In the absence of extracellular Ca^{2+},

oscillations in oxygen and glucose consumption cease. In the presence of 10 mM glucose, oxygen and glucose consumption remained stable when $[Ca^{2+}]_i$ was held constant. These data suggest that Ca^{2+} entry into islets is required for metabolic oscillations. Using modulators of $[Ca^{2+}]_i$, it was observed that during a transient increase in $[Ca^{2+}]_i$ oxygen consumption transiently increased and glucose consumption transiently decreased. Thus, a direct effect of $[Ca^{2+}]_i$ on metabolism was observed. Mitochondrial Ca^{2+} exchange is also discussed in Chapter 3. Inhibiting Ca^{2+} exodus from mitochondria through inhibition of the Ca^{2+}/Na^{+} exchanger resulted in generation of slow oscillations in oxygen consumption at islets only exhibiting fast oscillations. Disruption of the mitochondrial membrane potential, hindering Ca^{2+} entry into the mitochondria and oxidative phosphorylation, led to loss of oscillations in both oxygen and glucose consumption. Thus, mitochondrial Ca^{2+} exchange and intact oxidative phosphorylation are required for normal metabolic oscillations to occur.

Chapter 4 discusses the transport of glucose into the islets. Through monitoring the time necessary for extracellular glucose changes to reach the center of an islet transport into islets was investigated. It was observed that glucose equilibration into islets is not instantaneous. Inhibition of GK indicated that glucose metabolism slows the time of glucose equilibration into the islet. Changing Glut2 expression and glucose utilization by incubating islets in different concentrations of glucose showed that increased Glut2 expression and glucose utilization resulted in slower glucose equilibration in an islet. Decreasing extracellular Ca^{2+} levels also slowed the equilibration of glucose inside an islet. These data suggest that glucose equilibration

inside an islet is slowed by the transport of glucose into peripheral beta-cells and the metabolism of glucose in these cells.

In Chapter 5 other factors, which effect metabolism in islets, were investigated. It has been suggested that the increase in oxygen consumption rate in response to a glucose challenge at islets in the presence of Krebs Ringer Buffer (KRB), a salt solution not supplemented with amino acids, resulted from nutrient starvation instead of upregulation of GSIS [Pap98]. In Chapter 5, this claim was investigated through comparison of the change in oxygen level at islets during an increase in extra-islet glucose level in KRB and Dublecco's Modified Eagle Medium, an amino acid supplemented media. The oxygen level changed equivalently in both buffers; thus, the increase in oxygen level observed at islets in response to a glucose challenge is not the result of previous nutrient starvation. Chapter 5 also discusses the effect of knocking out IRS-1 receptors in murine islets on oscillations. It was found that islets from IRS-1 knock-out mice exhibited slow oscillations at a decreased rate as compared to wild mice of the same strain. This suggests that IRS-1 receptors are somehow involved in generation of slow oscillations; however, other aspects of oscillation propagation may have been affected in these knock-out mice. In Chapter 5 the effect of glucose incubation concentration on oscillations in glucose consumption is discussed. Glucose levels during incubation of islets modulate the expression and activity of Glut2 and glucose utilization. After islet incubation in low glucose levels, a decrease in Glut2 expression and reduction of glucose utilization occurs [Fer93, Ina92, Pur93, Yas92]. In the presence of 10 mM glucose, islets incubated at 11 mM glucose exhibited slow (n=6) or fast oscillations (n=1). Only half of the islets incubated in 2 mM glucose exhibited oscillations in oxygen level, the oscillations

observed were small amplitude fast oscillations in oxygen level. The islets incubated in 22 mM glucose exhibited very fast small amplitude oscillations (n=5) and slow oscillations (n=2). Thus, a change in Glut2 expression and glucose utilization can affect oscillations observed in islets.

Lastly, Chapter 6 discusses an improved Ru-O/CN-Ru microelectrode designed as a tool to study insulin secretion from single beta-cells. Modified microelectrodes have enabled secretion measurements from single canine and human beta-cells with good temporal resolution [Hua95, Ken93]. However, these microelectrodes are not sensitive enough for secretion measurements at single murine beta-cells. In Chapter 6, a method for improving the electrochemical plating procedure of Ru-O/CN-Ru is investigated. The electrochemical plating procedure presented gives increased sensitivity and stability of the Ru-O/CN-Ru layer; however, the sensitivity was not increased sufficiently for insulin secretion measurements from single murine beta-cells.

CHAPTER 2
EFFECT OF SUBSTRATE USED ON METABOLIC OSCILLATIONS

Introduction

Serum insulin and glucose levels oscillate with a period of 4 to 14 minutes in healthy individuals [Bal92, Eng95, Hun96, Lan79, Lan82, Ome93, Ora88, Pei92, Sto93, Por97]. Insulin oscillations account for 75% of insulin release in humans [Por97]. Type 2 diabetics and their close relatives often display erratic or non-existent pulsatility of serum insulin levels [Ora88], which has prompted studies to elucidate the chemical mechanism underlying oscillations in insulin secretion. Isolated islets of Langerhans also display pulsatility in insulin secretion, although with a faster period (0.5 to 3 min) [Bar96, Ber93, Ber94, Gil93].

According to the consensus model of glucose stimulated insulin secretion (GSIS) [Dee00, Hen00, Ish00, Kom97, Mat96, New95], glucose enters the beta cell through Glut2 transporters and is metabolized via glycolysis increasing ATP:ADP ratio, NADH and pyruvate levels. Pyruvate enters the mitochondria and is metabolized through the citric acid cycle. The reducing equivalents from NADH enter the mitochondria through either the malate-aspartate shuttle or the glycerol-3-phosphate shuttle. NADH and the products from the citric acid cycle enter oxidative phosphorylation, which utilizes oxygen and increases the ATP:ADP ratio [Duk94, Eto99a, Eto99b, Sch97]. The increase in ATP:ADP ratio closes ATP sensitive K^+ (K_{ATP}) channels, depolarizing the beta cell [Ash84, Coo84, Koh98] and opening voltage gated Ca^{2+} channels [Ror88]. The resulting increase in $[Ca^{2+}]_i$ initiates insulin secretion by exocytosis. Simultaneous measurement

of intracellular calcium concentration ($[Ca^{2+}]_i$) and insulin secretion suggests that pulses in $[Ca^{2+}]_i$ drive secretory pulses [Gil93].

Within this basic model, several possible feedback mechanisms exist, which could generate oscillations in $[Ca^{2+}]_i$ and insulin secretion. One possibility is that Ca^{2+} indirectly activates (opens) K_{ATP} channels; thus, preventing further $[Ca^{2+}]_i$ increases [Hen90]. Once $[Ca^{2+}]_i$ drops, K_{ATP} channels can be blocked once again increasing Ca^{2+} influx; thus, creating oscillations. Therefore, within this model, glucose metabolism is not involved. Another model holds that Ca^{2+} induces ATP consumption which decreases ATP levels; thus, providing feedback to membrane depolarization.

Another model suggests that oscillations in glycolysis entrain other processes in beta-cells and serve as a pacemaker for oscillations in insulin secretion [Tor75, Tor97]. Phosphofructokinase (PFK) exhibits both feedback inhibition and activation, making it a promising enzyme for oscillation generation [Tor97]. Studies using muscle cell extracts have shown PFK activity oscillates in response to changes in the concentration of cellular signals, including ATP:ADP ratio and fructose-1,6-biphosphate [Tor97]. Patients with defects in either PFK or GK have shown derangement in insulin pulsatility and predisposition to type 2 diabetes [Fro92, Hat92, Mah99, Per92, Vel97].

Evidence supporting the existence of metabolic oscillations at islets has been obtained. Mitochondrial membrane potential has been shown to oscillate in parallel to $[Ca^{2+}]_i$, with the depolarization actually happening in response to a change in $[Ca^{2+}]_e$, not glucose [Kri00]. Monitoring oxygen levels at a group of islets, single islets and single cells have revealed oscillations in oxygen consumption in all these preparations [Jun99a, Jun99b, Lon91, Ort00, Por00]. During the initial response to a glucose challenge oxygen

consumption increases prior to the increase in $[Ca^{2+}]_i$; however, during an oscillation changes in $[Ca^{2+}]_i$ precede changes in oxygen level by 1-2 s (with maximum $[Ca^{2+}]_i$ occurring during maximum oxygen consumption). Application of micro-sensors for monitoring glucose at single islets revealed that glucose consumption oscillates in phase with $[Ca^{2+}]_i$ oscillations at islets in response to a glucose challenge [Jun00]. $[Ca^{2+}]_i$, oxygen and glucose consumption exhibit three distinct types of oscillations, including slow oscillations, fast oscillations and slow oscillations with fast oscillations superimposed. In the absence of extracellular calcium the oscillations in oxygen [Jun99a] and glucose [Jun00] consumption at islets ceased, but oxygen consumption at clonal cells persisted with a decreased magnitude [Por00]. Thus, oscillations in metabolism occur at single cells and islets and depend on changes in $[Ca^{2+}]_i$.

In order to assess the role of different steps in metabolism in contributing to oscillations a study has monitored $[Ca^{2+}]_i$ oscillations in response to different fuels [Len00]. Of the fuels tested, only glucose could induce slow oscillations in $[Ca^{2+}]_i$. Alpha-ketoisocaproate (KIC), pyruvate and methyl pyruvate actually prevented these slow oscillations [Len00]. Only glucose could induce slow oscillations in $[Ca^{2+}]_i$. KIC, pyruvate and methyl pyruvate actually prevented these slow oscillations induced by glucose [Len00].

To further investigate the chemical mechanism underlying oscillations we have examined metabolic oscillations in response to different metabolites. Oxygen and glucose levels were monitored, using the newly developed sensors, to observe the response of an islet to glucose, GA, pyruvate, methyl pyruvate and KIC.

Experimental

Islet Isolation and Culture

Islets of Langerhans were isolated from mice pancreata using ductal injection of collagenase buffer (1 mg/mL) as described previously [Hua95] and in Appendix B. Islets were plated on nunc plates for microsensor experiments and on cover-slips for calcium measurements. Plates were incubated 2-4 days in RPMI 1640, containing 11 mM glucose, supplemented with 10% fetal bovine serum and 1% penicillin-streptomycin and placed in an incubator at 37°C humidified in 95% air and 5% CO_2.

Oxygen and Glucose Microsensor Fabrication and Measurements in Single Islets

Oxygen and glucose sensors were prepared as described previously [Jun99a, Jun99b, Jun00]. Refer to Appendix A for a detailed description of sensor manufacture. The oxygen microsensors are composed of 25 μm diameter platinum wire, with etched tips (3-9 μm), recessed into a glass pipette, sealed with epoxy and coated with cellulose acetate. Glucose sensors are similar to the oxygen sensors but before coating with cellulose acetate, platinum is plated into the recess and glucose oxidase is immobilized in the platinum matrix.

Plates containing islets were placed on a Zeiss Axiovert 35 microscope and perfused with modified Krebs-Ringer buffer (KRB) buffer containing 20 mM HEPES, 118 mM NaCl, 5.4 mM KCl, 2.4 mM Ca^{2+}, 1.2 mM $MgSO_4$, 1.2 mM KH_2PO_4, and 5 mM $NaHCO_3$ at 37°C. Using an insert the volume of the plates was reduced to 200 μL and under perfusion it took 24.8 s to completely change the buffer content. Oxygen was continuously flowed over the plates for glucose measurements. Microsensors were held at –0.6 V or 0.6 V, for oxygen and glucose respectively, versus Ag/AgCl reference electrode and inserted into the islet using Burleigh piezoelectric drivers (PCS-250).

Amperometric data were filtered at 20 Hz and acquired at 100 Hz using a digidata board from Axon Instruments and an IBM compatible personal computer.

Chemicals and Reagents

Platinum wire was obtained from Johnson Matthey, silver epoxy from Epoxy Technology, Inc., and epoxy from Miller-Stephenson Chemical Company. Reagents for culture media were purchased from Life Technologies, Inc. All other chemicals were obtained from Fisher or Sigma.

Results and Discussion

Potent insulin secretagogues include the fuels glucose, GA [Hel74] and KIC [Hut80b, Pan74]. Pyruvate, although readily oxidized by islets has not been shown to induce insulin secretion [Sen78]; however, methyl pyruvate can induce moderate levels of insulin secretion [Lem01, Mer96, Zaw97]. Table 2-1 shows a summary of oxygen

Table 2-1 Summary of oxygen consumption at single islets of Langerhans exposed to varying substrates.

Substrate	Concentration (mM)	Oxygen Level (%)[a]	Oscillations		
			Type	Period (s)	Magnitude (mmHg)
Glucose	10	89 ± 3	slow	197 ± 10	3.3 ± 0.3
			fast	17 ± 3	1.2 ± 0.1
Glyceraldehyde	5	91 ± 2	fast	25 ± 3	1.6 ± 0.5
	10	89 ± 4	fast	22 ± 3	1.0 ± 0.1
KIC	5	95 ± 2	fast	33 ± 3	0.54 ± 0.04
	10	89 ± 3			
Pyruvate	10	102 ± 1	no oscillations		
	20	104 ± 1			
Methyl Pyruvate	10	98 ± 1	no oscillations		
	20	97 ± 1			

a Oxygen level given as percentage of oxygen level at 0 mM substrate.

levels and oscillations observed at islets in response to the metabolic fuels tested. In this study we found that only potent insulin secretagogues were capable of inducing oscillations in metabolism, indicating a relationship between the ability to induce oscillations in metabolism and insulin secretion. Stimulatory levels of glucose and a combination of low glucose with GA were the only fuels able to induced slow oscillations in oxygen levels. Fast oscillations were generated in response to glucose, GA, and KIC.

Glyceraldehyde and Metabolic Oscillations

D-Glyceraldehyde (GA) enters freely into the islets and can cause insulin secretion at beta-cells and islets [Hel74, Ash73]. Exposure to high concentrations of GA for an hour or low concentrations of GA for a day can harm beta cells [Mac89]; thus, we limited exposure to GA to less than 1 h. GA can induce oscillations in oxygen level at a much lower concentration of GA (2-3 mM) than glucose (7 mM) (data not shown). Only fast oscillations were observed in the presence of GA (Fig. 2-1), which were similar in magnitude to fast oscillations observed with 10 mM glucose, although the period was somewhat slower (Table 2-1).

The exact mechanism of GA metabolism in beta-cells is unknown; however, three mechanisms have been proposed. GA can be converted into glyceraldehyde-3-phosphate (G3P) by triose kinase, which has a K_m of 8-35 μM for GA [Fra71, Sil69]. G3P can either enter glycolysis through conversion into 1,3-bisphosphoglycerate by glyceraldehyde-3-phosphate dehydrogenase or G3P can be converted into glycerol-3-phosphate by triose phosphate isomerase and feed into the glycerol-3-phosphate shuttle. Both of these pathways will lead to an increase in the reducing equivalents entering the mitochondria; thus, increasing oxygen consumption. An alternative pathway for GA

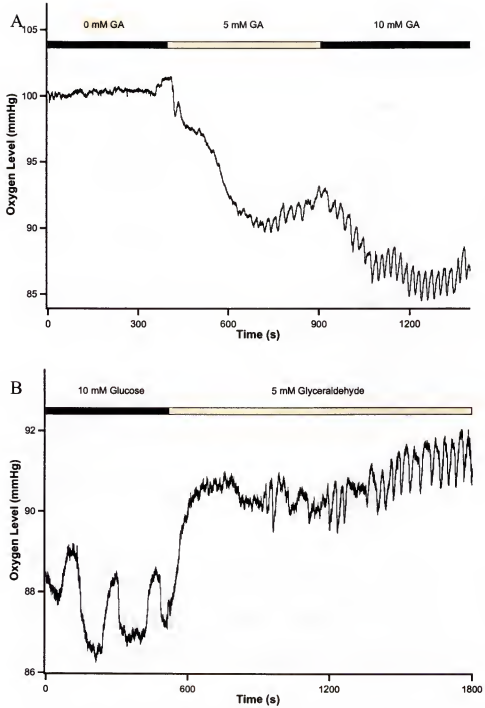

Figure 2-1 Oxygen consumption exhibits fast oscillations at islets in response to GA. (A) Oxygen consumption increases (shown as a decrease in oxygen level) and fast oscillations develop at an islet in response to increasing levels of GA. (B) An islet exhibiting slow oscillations in oxygen consumption in response to 10 mM glucose develops fast oscillations when the glucose is replaced by 5 mM GA. When 10 mM GA was used instead of 5 mM GA fast oscillations still developed out of the slow oscillations observed with 10 mM glucose (data not shown).

metabolism consists of GA conversion into glyceraldehyde-1-phosphate (G1P) by glyceraldehyde-phosphate dehydrogenase [Mac89]. Although the initial conversion step of GA to G1P, produces one NADH, there is no known metabolism of G1P or glyceric acid, which is the most likely degradation product of G1P, in the beta cell Thus, G1P and/or glyceric acid, would build up in the beta cells. If this were the dominant pathway for GA metabolism, we would expect an initial increase in oxygen consumption but then a drop as G1P and the degradation products build up. Instead, a continual elevated level of oxygen consumption was observed in islets in response to GA, similar to what is observed with 10 mM glucose. Second, glyceraldehyde-phosphate dehydrogenase has a K_m of 4.8 mM for GA, but oscillations were observed at much lower concentrations of GA. This data suggests that during limited exposure (<60 min.) of islets to 10 mM GA, the GA is converted by triose kinase into G3P, which is further metabolized by glycolysis.

Ketoisocaproate and Metabolic Oscillations

KIC enters metabolism in the mitochondria through the citric acid cycle; thus, producing less ATP per carbon than glucose; however, KIC is a more potent insulin secretagogue than glucose. The increased insulin secretion is believed to be the result of both KIC metabolism and a direct interaction between KIC and the K_{ATP} channel [Bra98]. Thus, KIC can depolarize beta cells without the production of large quantities of ATP.

Figure 2-2 shows that changing fuels from 10 mM glucose to 5 mM KIC induced a large transient increase in oxygen consumption. Following the transient increase in oxygen consumption the oxygen level returned to that observed in the presence of 10 mM

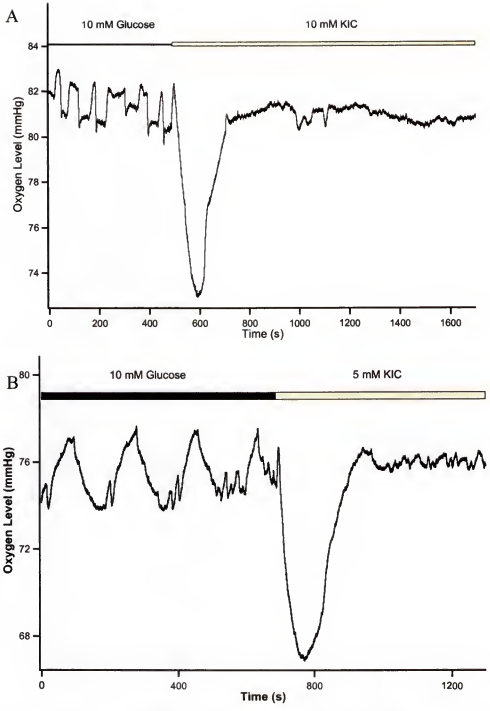

Figure 2-2 Oxygen consumption at islets in response to KIC. (A) When 10 mM glucose is replaced with 5-10 mM KIC an initial large burst of oxygen consumption occurs; however, oscillations cease. (B) When an islet incubated with Fura-2 (ionophore utilized for $[Ca^{2+}]_i$ measurements) replacing 10 mM glucose with 5 mM KIC results in the development of irregular fast oscillations in oxygen consumption.

glucose. This data suggests that initially KIC up-regulates mitochondrial metabolism but is not capable of maintaining this high level of metabolism for an extended time.

Comparing Figure 2-2A and B shows that in the absence of fura-2 loading, no oscillations were observed in oxygen consumption; however, in the presence of fura-2 oscillations in oxygen consumption were observed. Fura-2 is a fluorescent dye utilized for measurements of $[Ca^{2+}]_i$ and by binding to Ca^{2+} may amplify changes in $[Ca^{2+}]_i$. During the increases in Ca^{2+} influx, which occur during oscillations, fura-2 will bind the Ca^{2+}, which could slow the action of Ca^{2+} within the beta-cells. Thus, the possible effects of Ca^{2+} within the cell, which lead to decreases in Ca^{2+} influx, could be delayed, giving rise to a larger increase in $[Ca^{2+}]_i$ than would otherwise be observed. The effect of fura-2 on oxygen oscillations is indicative of a direct effect of $[Ca^{2+}]_i$ on oxygen consumption and suggests that fast oscillations observed in metabolism are induced by changes in $[Ca^{2+}]_i$.

In the present study 10 mM KIC produced a similar decrease in oxygen level as 10 mM glucose (Table 2-1). However, even in the presence of fura-2, the magnitude of fast oxygen oscillations was much smaller than that observed in response to 10 mM glucose. KIC is capable of increasing metabolism of glutamate and islets contain a sufficient store of glutamate to allow for a high rate of respiration for at least 2 h [Lem98]. Therefore, an increased amount of oxygen can be consumed relative to the ATP produced as compared to glucose induced oxygen consumption. The decreased oscillation magnitude in oxygen consumption may be due to the direct effect of KIC on K_{ATP} channels, which could amplify changes in $[Ca^{2+}]_i$ during metabolic oscillations.

Pyruvate and Methyl Pyruvate Metabolism

Pyruvate is metabolized within the mitochondria through the citric acid cycle to produce an increase in the ATP:ADP ratio. Figure 2-3 shows that oscillations in oxygen consumption in response to 10 mM glucose ceased when glucose was replaced by 20 mM pyruvate. It has been shown that some substrates, although oxidized within an islet, do not increase oxygen consumption at an equivalent rate, which has been associated with the inability of a substrate to induce insulin secretion [Hut80a]. This may explain why pyruvate, which is readily oxidized within an islet [Gun73, Hed72, Liu71, Mal79, Sen78], is not insulinotropic on its own [Mer96, Sen78, Zaw97].

There is also some concern that pyruvate is not membrane permeable (although the oxidation of pyruvate in intact islets should negate this belief). Therefore, an alternative to pyruvate, methyl pyruvate, which can freely pass through the cell membrane, has been utilized. Once inside the cell the methyl group can be removed by an esterase to form pyruvate. Figure 2-4 shows the effect of changing from 10 mM glucose to 20 mM methyl pyruvate. The oxygen level at an islet was much higher in the presence of methyl pyruvate than glucose (Table 2-1); however, methyl pyruvate was able to increase oxygen consumption, whereas pyruvate could not. Oscillations present in oxygen consumption in response to 10 mM glucose cease when 20 mM methyl pyruvate was applied, as shown in Figure 2-4. This may result from the higher rate of mitochondrial metabolism of methyl pyruvate versus pyruvate [Jij96], which may also account for the ability of methyl pyruvate, unlike pyruvate, to initiate insulin secretion within an islet [Jij96, Mer96, Zaw97]. Previously it has been shown that the second phase insulin release potentiated by methyl pyruvate was substantially lower than that

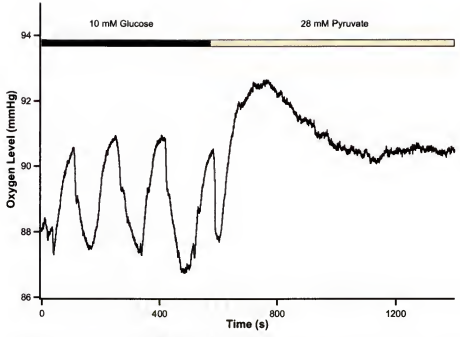

Figure 2-3 Oxygen consumption at an islet in response to pyruvate. Slow oscillations in oxygen consumption in response to glucose ceased when 10 mM glucose was replaced with 20 or 28 mM pyruvate. No oscillations were observed in response to pyruvate and the oxygen level was similar to that seen in the absence of any substrate.

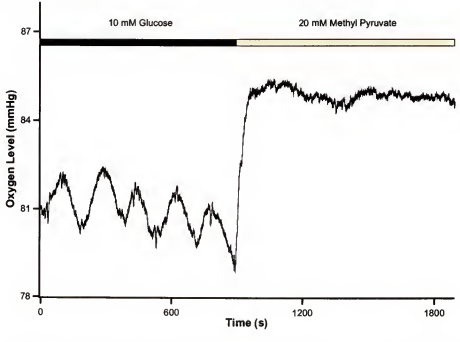

Figure 2-4 Effect of methyl pyruvate on oxygen consumption. An islet initially oscillating in the presence of 10 mM glucose ceased to oscillate in response to 20 mM pyruvate. The oxygen level in response to methyl pyruvate increased as compared to 10 mM glucose, but was lower than that observed without any substrate present.

evoked by glucose [Mer96, Zaw97]. Our data support this since 20 mM methyl pyruvate did not increase oxygen consumption to the same degree as 10 mM glucose.

Slow Versus Fast Oscillations

Figure 2-5 shows the three different types of oscillations observed in oxygen and glucose level in response to 10 mM glucose; slow oscillations, fast oscillations, and fast oscillations superimposed on slow oscillations. The fast oscillations superimposed on slow oscillations observed in oxygen consumption resemble oscillations in oxygen flux at beta-cells predicted by a recent model of beta-cell mitochondrial activity [Mag98]. When exposing islets to only one substrate at a time slow oscillations in oxygen level were only observed in the presence of stimulatory levels of glucose (Fig 2-5). This observation is in agreement with a recent report, which showed that slow oscillations in $[Ca^{2+}]_i$ could only be observed in the presence of glucose [Len00]. This result suggests that slow metabolic oscillations require metabolic flux through glycolysis. It is reasonable to speculate that a glycolytic enzyme, such as PFK, could control these oscillations either through spontaneous oscillation in the enzyme activity as described by Tornheim or through modulation of the enzyme activity by changes in ATP/ADP brought on by Ca^{2+} entry into the cell.

In the presence of 3 mM glucose and 5 mM GA slow oscillations were observed in glucose (Figure 2-6) and oxygen levels. Figure 2-7 shows the three different patterns of oscillations observed in glucose levels in response to 3 mM glucose and 5 mM GA. These results are indicative of GA potentiation on the effect glucose has on beta-cell metabolism which causes slow oscillations.

Fast oscillations in oxygen consumption were observed in islets stimulated with GA and KIC (in the presence of fura-2); however, neither pyruvate nor methyl pyruvate

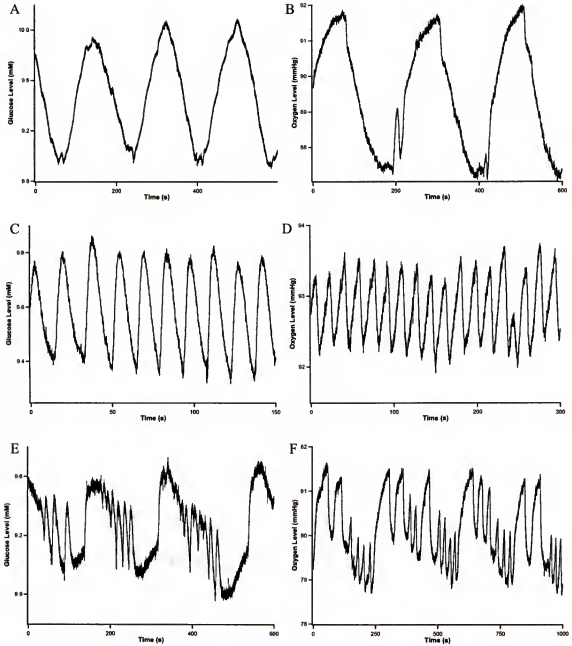

Figure 2-5 Oscillatory patterns in glucose and oxygen consumption in response to 10 mM glucose. Slow oscillations in glucose (A) and oxygen (B) consumption exhibit an average period of 197 +/- 10 s. at single islets. Average periods of 17 +/- 3 s. are monitored at oscillations in glucose (C) and oxygen (D) consumption. Fast oscillations superimposed on slow oscillations can also be observed in glucose (E) and oxygen (F) consumption.

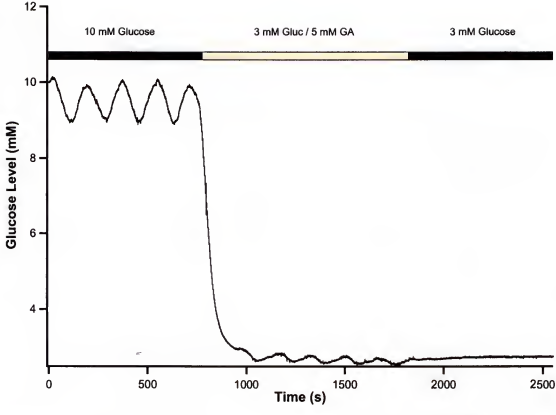

Figure 2-6 Slow oscillations in glucose consumption observed in response to 3 mM glucose and 5 mM GA. While monitoring glucose consumption at an islet exposed to 10 mM glucose and exhibiting slow oscillations, the slow oscillations persist when GA is introduced to the islet in combination with non-stimulatory levels of glucose. Oscillations are lost upon removal of GA.

were able to induce oscillations in oxygen consumption. These data suggest that fast oscillations in metabolism are induced by changes in Ca^{2+}, not glucose metabolism.

Conclusions

We have shown that in response to a single substrate slow oscillations in glucose and oxygen consumption occur only in the presence of stimulatory levels of glucose. Through potentiation of the glucose effect on beta-cells GA is able to induce slow oscillations in oxygen and glucose consumption if combined with below stimulatory levels of glucose. KIC, pyruvate and methyl pyruvate are unable to induce slow oscillations in oxygen consumption. Therefore, we propose that slow oscillations

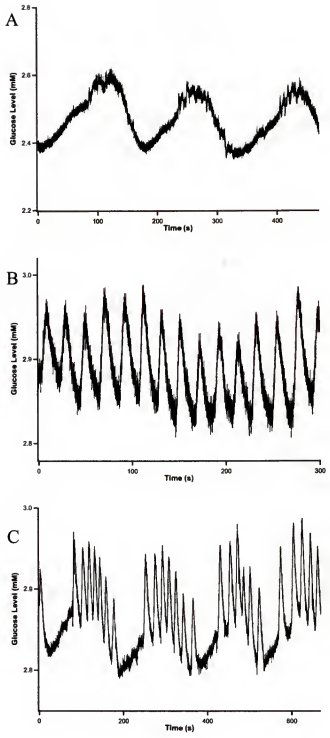

Figure 2-7 Oscillation patterns observed in glucose consumption in response to 3 mM glucose and 5 mM GA; slow (A), fast (B) and fast superimposed on slow (C).

observed in islets are mediated by inherent glycolytic oscillations. The data presented suggest that the slow oscillations are generated at glycolytic enzymes, and are sensitive to levels of products, substrates, ATP:ADP ratio and/or extracellular Ca^{2+} levels. It is possible that these oscillations are modified by glucose entry into the islet through Glut 2 transporters, but as of yet there are no reports of direct regulation of Glut 2 by cellular signals.

GA and KIC (in the presence of fura-2) were able to induce fast oscillations in oxygen consumption. Since fast oscillations could be observed in conditions where slow oscillations were not monitored, we propose that different mechanisms underlie the two types of oscillations. We suggest that the fast oscillations in oxygen consumption are the result of changes in $[Ca^{2+}]_i$.

CHAPTER 3
INTRACELLULAR CALICUM MODIFIERS AND METABOLIC OSCILLATIONS

Introduction

Insulin secretion, $[Ca^{2+}]_i$, oxygen and glucose consumption oscillate in single islets of Langerhans in response to a glucose challenge [Bar96, Ber93, Ber94, Gil93, Jun99a, Jun99b, Jun00, Ort00]. These oscillations are believed to be the source of blood insulin pulsatility in normal individuals [Lan79, Lan82, Ora88, Pei92], which are altered in individuals with type 2 diabetes [Ora88]. Thus, a substantial amount of research has focused on finding the underlying cause of these oscillations.

In response to a glucose challenge beta cells release insulin enabling glucose homeostasis to be maintained. The consensus model of glucose stimulated insulin secretion (GSIS) [Kom97, Mat96, New95] involves glucose entry into the beta cell through Glut 2 transporters. Glucose is then metabolized through glycolysis producing an elevated ATP:ADP ratio, NADH and pyruvate levels [Duk94, Eto99a, Eto99b, Sch97]. Pyruvate enters the mitochondria and is metabolized through the citric acid cycle. The reducing equivalents from NADH enter the mitochondria through either the malate-aspartate shuttle or the glycerol-3-phosphate shuttle. NADH (from glycolysis and the citric acid cycle) and succinate (during a step in the citric acid cycle) donate electrons to the respiratory chain, which enable proton transport out of the mitochondria creating the proton motive force. At the last phosphorylation site the electrons are transferred to oxygen, which is converted, with 2 protons, into water. Using the proton motive force, ATP-synthase converts ADP to ATP. The increased ATP:ADP ratio closes K_{ATP}

channels, which depolarize the cell [Ash84, Coo84, Koh98]. Cell depolarization opens voltage-gated calcium channels increasing $[Ca^{2+}]_i$ and subsequently triggering exocytosis [Ror88]. These steps are believed to oscillate in respect to each other but the causative factors underlying the oscillations are unknown.

Although the triggers of oscillations in cellular activities within the islet are still unknown, two models, consistent with GSIS, have been proposed. One model is based on the inherent oscillatory behavior of glycolysis [Tor97]. The inherent oscillations observed in glycolysis have been proposed as a pacemaker for oscillations in insulin secretion. Another model proposes the regulation Ca^{2+} entry into beta-cells, in response to K_{ATP} channel conductance, as the basis of oscillations [Hen90]. This model proposes that the increase in $[Ca^{2+}]_i$ increases ATP usage through triggering exocytosis and other energy utilizing cellular activities. This leads to a decrease in ATP:ADP ratio, which reopens K_{ATP} channels, decreasing Ca^{2+} entry. The decrease in $[Ca^{2+}]_i$ leads to a decrease in ATP usage, increasing ATP:ADP ratio [Gil02, Hen90, Rol02]. Thus, through affecting ATP levels within the cell, $[Ca^{2+}]_i$ mediates oscillations.

Recently observations of other cellular analytes have shown the existence of metabolic oscillations. Oscillations in mitochondrial membrane potential have been monitored [Kri00]. These oscillations were shown to be dependent on changes in cytosolic Ca^{2+} concentration, and not changes in glucose level [Kri00]. Utilizing sensors capable of detecting changes in oxygen and glucose levels in micro-environments, oscillations in oxygen and glucose consumption at single islets have been observed [Jun99b, Jun00]. These sensors have allowed for simultaneous measurements of oxygen or glucose level while monitoring $[Ca^{2+}]_i$. It was found that, although during the initial

response to a glucose challenge changes in oxygen level preceded changes in $[Ca^{2+}]_i$, after the initial reaction to glucose subsided changes in oxygen consumption follow changes in $[Ca^{2+}]_i$ (with maximum $[Ca^{2+}]_i$ occurring during maximum oxygen consumption) [Jun00]. Simultaneous measurements of $[Ca^{2+}]_i$ and glucose levels showed that during oscillations, changes in $[Ca^{2+}]_i$ led changes in glucose level [Jun00]. This indicates that, although glucose metabolism is paramount in triggering initial $[Ca^{2+}]_i$ changes, $[Ca^{2+}]_i$ leads oscillations in metabolism when ample energy is present.

To further investigate the chemical mechanism underlying metabolic oscillations we have monitored metabolism at islets in response to modulators of $[Ca^{2+}]_i$ and mitochondrial Ca^{2+} exchange. Oxygen and glucose levels were monitored in response to changes in extracellular Ca^{2+} levels, K_{ATP} channel blockers and activators. The effect of inhibiting mitochondrial Na^+-Ca^{2+} exchanger and collapsing mitochondrial membrane potential, which affects both oxidative respiration and Ca^{2+} transport into the mitochondria, was also investigated.

Experimental

Islet Isolation and Culture

Islets of Langerhans were isolated from mice pancreata using ductal injection of collagenase buffer (1 mg/mL) as described previously [Hua95]. Islets were plated on nunc plates for microsensor experiments and incubated 2-4 days in RPMI 1640, containing 11 mM glucose, supplemented with 10% fetal bovine serum and 1% penicillin-streptomycin and placed in an incubator at 37°C humidified in 95% air and 5% CO_2.

Oxygen and Glucose Microsensor Fabrication and Measurements in Single Islets

Oxygen and glucose sensors were prepared as described previously [Jun99a, Jun99b, Jun00]. Refer to Appendix A for detailed description of microsensor manufacture. The oxygen microsensors are composed of 25 μm diameter platinum wire, with etched tips (3-9 μm), recessed into a glass pipette, sealed with epoxy and coated with cellulose acetate. Glucose sensors are similar to the oxygen sensors but before coating with cellulose acetate, platinum is plated into the recess and glucose oxidase is immobilized in the platinum matrix.

For detailed description of islet isolation procedure and Amperometric setup refer to Appendices B and C. Plates containing islets were placed on a Zeiss Axiovert 35 microscope and perfused with modified Krebs-Ringer buffer (KRB) buffer containing 20 mM HEPES, 118 mM NaCl, 5.4 mM KCl, 2.4 mM Ca^{2+}, 1.2 mM $MgSO_4$, 1.2 mM KH_2PO_4, and 5 mM $NaHCO_3$ at 37°C. Using an insert the volume of the plates was reduced to 200 μL and under perfusion it took 24.8 s to completely change the buffer content. Oxygen was continuously flowed over the plates for glucose measurements. Microsensors were held at –0.6 V or 0.6 V, for oxygen and glucose respectively, versus Ag/AgCl reference electrode and inserted into the islet using Burleigh piezoelectric drivers (PCS-250). Amperometric data were filtered at 20 Hz and acquired at 100 Hz using a digidata board from Axon Instruments and an IBM compatible personal computer.

Chemicals and Reagents

Platinum wire was obtained from Johnson Matthey, silver epoxy from Epoxy Technology, Inc., and epoxy from Miller-Stephenson Chemical Company. FCCP and

CGP 37157 were acquired from Tocris, and reagents for culture media from Life Technologies, Inc. All other chemicals were obtained from Fisher or Sigma.

Results and Discussion

Ca^{2+} is a secondary messenger in many biological systems and is directly involved in exocytosis of hormones, such as insulin. Intracellular Ca^{2+} concentrations ($[Ca^{2+}]_i$) have been found to oscillate in many cell types; however, the exact role of $[Ca^{2+}]_i$ in regulating metabolic oscillations is not known. Previously we have shown that during oscillations at islets, the changes occurring in $[Ca^{2+}]_i$ precede changes in both oxygen and glucose consumption [Jun00], suggesting that $[Ca^{2+}]_i$ may have a regulatory role in oscillation generation.

Extracellular Calcium

Studies have shown that exclusion of Ca^{2+} from extracellular medium prevents the development of oscillations in oxygen and glucose consumption [Jun00] at single islets. However, there have also been reports of oscillations in insulin secretion [We96, Wes97] and oxygen level [Ber93, Ber94] in the absence of extracellular Ca^{2+}. These oscillations have recently been attributed to the use of aged ob/ob mice [Kje02]. It was found that beta-cells from young NMRI, lean and ob/ob mice showed no pulsatility in insulin secretion in the presence of stably elevated $[Ca^{2+}]_i$; however, some beta-cells from older mice (10 months) display oscillations in insulin secretion under the same conditions [Kje02]. The oscillations observed during stably elevated $[Ca^{2+}]_i$ were more common in ob/ob mouse beta-cells and had a much smaller amplitude than oscillations in insulin secretion induced by oscillations in $[Ca^{2+}]_i$ [Kje02]. Figure 3-1 shows the effect of removing extracellular Ca^{2+} from an islet oscillating in the presence of 10 mM glucose. Initially experiments were performed with 0.0 mM extracellular Ca^{2+}; however, islets

disintegrated under these conditions. Thus, further experiments were performed in the presence of 0.1 mM Ca^{2+}. Without extracellular Ca^{2+} neither glucose nor oxygen consumption oscillate. In absence of extracellular Ca^{2+}, membrane depolarization induced by closure of in K_{ATP} channels during a glucose challenge is unable to cause an influx of Ca^{2+}. Thus, the data suggests that metabolic oscillations require the entry of Ca^{2+}.

Upon removal of extracellular Ca^{2+} the oxygen level monitored in islets increased as shown in Figure 3-1. The increase in level indicates a decrease in consumption of oxygen by the islet. Thus, the amount of oxygen consumed in response to 10 mM glucose was much lower in the absence of extracellular Ca^{2+} (Table3-1). Ca^{2+} activates cellular processes, such as insulin secretion, which utilize ATP resulting in upregulation of glycolysis. The increased rate of glycolysis, combined with direct activation of mitochondrial dehydrogenases by Ca^{2+}, increases oxygen usage through oxidative phosphorylation. Thus, it is not surprising that under conditions where extracellular Ca^{2+} levels are depleted oxygen and glucose consumption are decreased.

Table 3-1 Effect of extracellular Ca^{2+} on oxygen level at an islet exposed to 20 mM glucose.

Extracellular Calcium (mM)	Oxygen Level (%)[a]
2.45	86 ± 1[b]
0.10	96 ± 2[b]

a Oxygen level given as percentage of oxygen level at 3 mM substrate.
b Oxygen levels are significantly different, p=0.01 (98% confidence).

Pulsing K+

The beta-cell membrane potential is primarily controlled by K_{ATP} channel activity. During glucose stimulation the membrane is depolarized by closure of K_{ATP} channel in response to increased ATP:ADP ratio, resulting in the opening of voltage gated Ca^{2+}

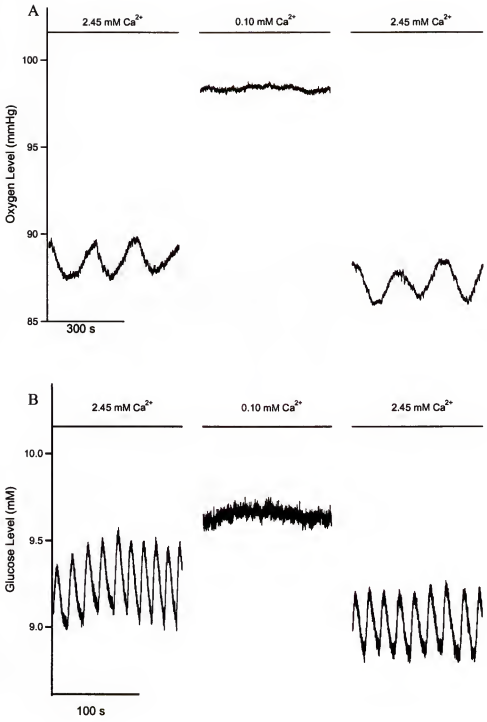

Figure 3-1 Effect of removing extracellular Ca^{2+} from an islet oscillating in response to 10 mM glucose. Neither oxygen level (A) nor glucose level (B) continued to oscillate once extracellular Ca^{2+} was removed. However, when extracellular Ca^{2+} was reintroduced, metabolic oscillations resumed.

channels, which increases $[Ca^{2+}]_i$. Membrane depolarization can be achieved by increasing extracellular K^+ concentration. Increasing extracellular K^+ level results in a transient increase in $[Ca^{2+}]_i$ followed by steady state elevated $[Ca^{2+}]_i$ [Jon98, Hen90, Rav99]. Returning extracellular K^+ to normal levels results in a decrease in $[Ca^{2+}]_i$ to levels observed before the K^+ pulse [Jon98, Hen90, Rav99]. Figure 3-2A shows the effect of pulsing extracellular K^+ levels on oxygen and glucose consumption. Oxygen consumption increases rapidly in response to the increase in K^+ but then drops to a steady state value. After K^+ levels are returned to normal, oscillations in oxygen consumption resumed, as expected at 10 mM glucose. The pattern of oxygen consumption in response to a pulse in K^+ resembles that observed in $[Ca^{2+}]_i$, with the maximum oxygen consumption occurring during maximum $[Ca^{2+}]_i$. This parallels the relationship between oxygen consumption and $[Ca^{2+}]_i$ observed during simultaneous monitoring of the analytes during oscillations. Figure 3-2B shows that glucose consumption was inhibited in response to the increased extracellular K^+. However, the glucose consumption returns to previous levels after a short period, in conjunction with the decrease in $[Ca^{2+}]_i$ observed after the initial burst of Ca^{2+} influx. These data suggest that the transient increase in $[Ca^{2+}]_i$ caused by membrane depolarization directly affects cellular activity, such as glucose and oxygen consumption. This is indicative of strong involvement of $[Ca^{2+}]_i$ in the oscillatory activity of beta-cells.

Diazoxide

Diazoxide blocks K_{ATP} channels in the open position, preventing glucose induced membrane depolarization and Ca^{2+} entry into beta-cells [Gem93, Gil93]. Previous

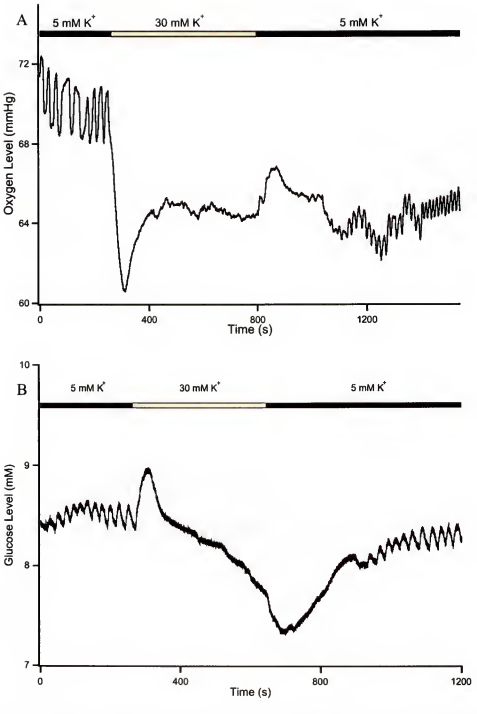

Figure 3-2 Effect of pulsing extra-islet K^+ on oxygen (A) and glucose (B) level at an islet in the presence of 10 mM glucose. A decrease in level represents an increase in consumption at an islet. Islets exhibiting oscillations in oxygen and glucose consumption in response to 10 mM glucose showed a transient increase in oxygen consumption and a transient decrease in glucose consumption in response to increased K^+ level. After return of extra-islet K^+ to normal levels, oscillations in oxygen and glucose consumption resumed.

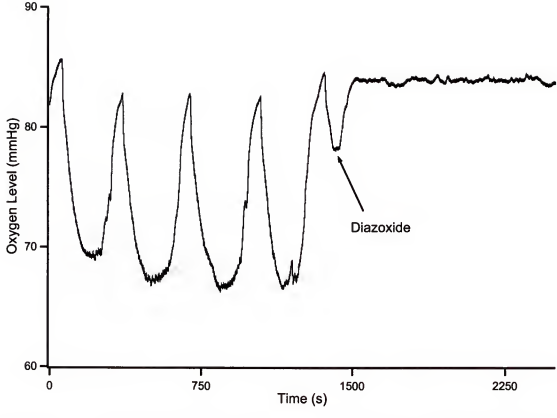

Figure 3-3 Oxygen level at an islet in response to diazoxide. Application of 150 μm diazoxide inhibited slow oscillations in oxygen level observed at an islet in response to 10 mM glucose. The oxygen level remained relatively high during exposure to diazoxide. [Reproduced with permission from Ken02]

research has shown that exposure of an islet stimulated with 15 mM glucose to diazoxide resulted in inhibition of oscillations in $[Ca^{2+}]_i$ and insulin secretion [Gil93]. Figure 3-3 shows the effect of diazoxide on oxygen consumption. Oscillations in oxygen consumption observed in the presence of 10 mM glucose ceased upon the addition of diazoxide. Thus, indicating that metabolic oscillations require changes in K_{ATP} conductance to occur. It was also observed that the oxygen level in the islets remained relatively high during exposure to diazoxide. This is indicative of a decrease in metabolism during decreased Ca^{2+} entry into the beta-cells. These data support the data observed during removal of extracellular Ca^{2+}.

Diazoxide and Pulsing K^+

Utilizing diazoxide in conjunction with K^+ allows for control of membrane potential and, which allows for control over Ca^{2+} entry. After observing oscillations in response to 10 mM glucose, diazoxide in the presence of 5 or 30 mM K^+ was perfused over the islets. Holding the K_{ATP} channels open with diazoxide in the presence of 5 mM K^+ holds the membrane polarized, increasing K^+ to 30 mM will depolarize the membrane potential. Figure 3-4 shows the effect of pulsing K^+ in the presence of 10 mM glucose and diazoxide on islet oxygen and glucose consumption. A transient increase in oxygen consumption occurred in response to an increase in extracellular K^+, similar to that observed in the absence of diazoxide. During exposure to diazoxide, the oxygen level observed in response to normal K^+ level was much higher than that observed in response to elevated K^+. This data suggests that during elevated K^+ levels, while $[Ca^{2+}]_i$ is high, oxygen consumption is increased, possibly due to activation of mitochondrial dehydrogenases. When K^+ was decreased back to 5 mM, oxygen consumption did not oscillate, due to the presence of diazoxide. The increase in extra-islet K^+ levels evokes a transient decrease in glucose consumption. During the decrease of K^+ to normal levels, a transient decrease in glucose consumption was observed in some islets; however, this transient change is much smaller in amplitude than that observed during the initial increase in extra-islet K^+. The level of glucose does not show a change comparable to the change observed in oxygen level, which indicates that steady $[Ca^{2+}]_i$ does not directly change the rate of glycolysis. Thus, polarization of membrane potential is accompanied by a pulse of increased oxygen consumption and decreased glucose consumption, under conditions where $[Ca^{2+}]_i$ is allowed to increase.

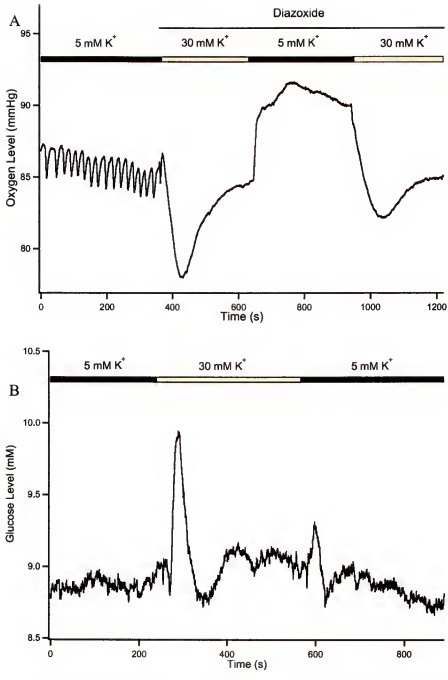

Figure 3-4 Effect of pulsing K^+ levels in the presence of 150 μM diazoxide and 10 mM glucose on oxygen (A) and glucose (B) level. Consumption increases with decreasing level. (A) Oxygen level oscillated at an islet initially exposed to 10 mM glucose, upon introduction of diazoxide and 30 mM K^+ a transient increase in oxygen consumption was observed. (B) Glucose level at an islet initially in the presence of 10 mM glucose and 150 μm diazoxide. During pulses of 30 mM K^+ a decrease in glucose consumption was observed. No oscillations in oxygen or glucose consumption were observed in the presence of diazoxide.

Mitochondrial Ca^{2+} Exchange

It has been proposed that bursts in beta cell membrane potential, seen with stimulatory levels of glucose, are induced by mitochondrial Ca^{2+} exchange [Kri00]. During oscillations the increase in $[Ca^{2+}]_i$ increases Ca^{2+} influx into the mitochondria, potentially depolarizing the inner mitochondrial membrane and decreasing the rate of mitochondrial ATP production. Therefore, the cytosolic ATP:ADP ratio would decrease, opening K_{ATP} channels and closing the voltage gated Ca^{2+} channels. Closing the Ca^{2+} channels would decrease $[Ca^{2+}]_i$ and allow for an eventual repolarization of the inner mitochondrial membrane increasing the rate of ATP production, closing K_{ATP} channels, and; thus, completing an oscillatory cycle. To investigate the effect mitochondrial Ca^{2+} exchange, the mitochondrial Na^{+}-Ca^{2+} exchanger and Ca^{2+} influx were separately inhibited.

Mitochondrial Na^{+}-Ca^{2+} Exchanger

The mitochondrial Na^{+}-Ca^{2+} exchanger transports Ca^{2+} from the mitochondria to the cytosol. CGP 37157 specifically inhibits this exchanger. Figure 3-5 shows the effect of 8 μM CGP 37157 on oscillations observed in oxygen consumption at an islet in response to 10 mM glucose. Fast (n=4) or unstable (n=1) oscillations in oxygen consumption monitored at an islet became more slow oscillations, often with fast oscillations superimposed, in response to CGP 37157. Islets exhibiting slow oscillations in oxygen consumption showed no change in oscillation period in response to CGP 37157 (n=3). This suggests a connection between mitochondrial Ca^{2+} exchange and fast oscillations. Through inhibiting Ca^{2+} efflux from the mitochondria, mitochondrial Ca^{2+} concentration ($[Ca^{2+}]_m$) would remain elevated independent of changes in $[Ca^{2+}]_i$. During oscillations the increase in $[Ca^{2+}]_i$ would not be able to increase mitochondrial

dehydrogenase activity through increases in $[Ca^{2+}]_m$. Thus, oxygen consumption is no longer directly modulated by $[Ca^{2+}]_i$, suggesting that slow oscillations in oxygen consumption are not caused by a direct effect of changes in $[Ca^{2+}]_i$ on oxygen consumption.

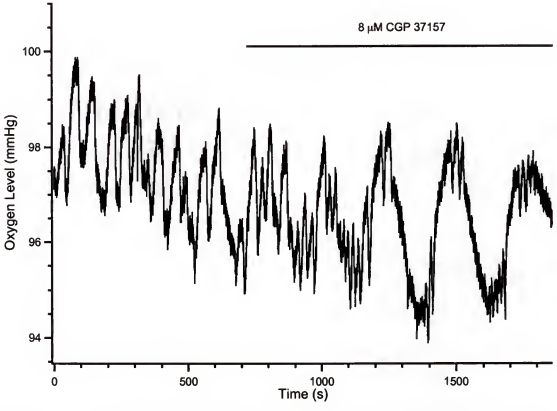

Figure 3-5 Oscillations in oxygen level at an islet exposed to 10 mM glucose are transformed into slow oscillations in the presence of 8 mM CGP 37157.

Mitochondrial Ca^{2+} Influx

Carbonyl cyanide 4- (trifluoromethoxy) phenyl hydrazone (FCCP) uncouples the proton motive force, through transporting protons into the mitochondria, resulting in a collapse of the mitochondrial membrane potential. This blocks the Ca^{2+} influx into the mitochondria through the uniporter and decreases the efficiency of ATP produced during oxidative phosphorylation. To compensate for the decrease in the proton motive force

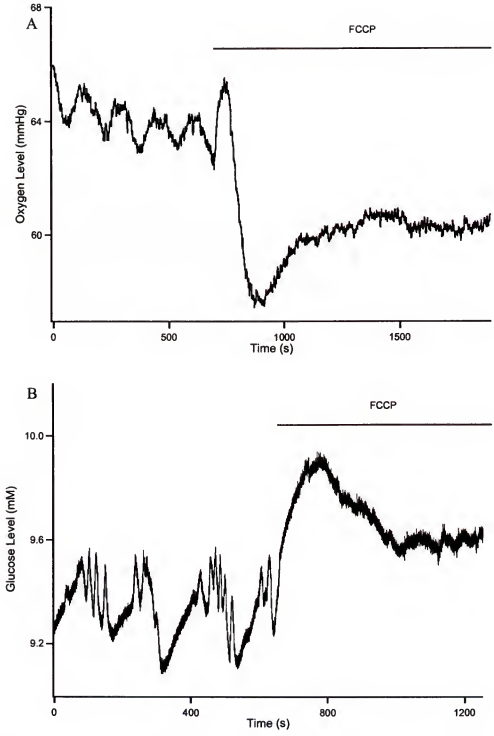

Figure 3-6 Effect of 1 μM FCCP on oxygen (A) and glucose (B) level in the presence of 10 mM glucose. Oscillations in oxygen and glucose level ceased after application of FCCP. (A) Oxygen level transiently decreased in response to FCCP. (B) Glucose level transiently increased in response to FCCP.

the rate of oxidative phosphorylation will increase. Figure 3-6 shows the effect of FCCP on oxygen and glucose consumption. Oscillations in oxygen and glucose consumption in response to 10 mM glucose cease in response to 1 μm FCCP. Thus, the mitochondrial membrane potential is required to be intact for metabolic oscillations to occur. In response to FCCP a transient increase in oxygen consumption occurs, which decreases after a few minutes; however, the oxygen consumption remains elevated in the presence of FCCP. This increase in oxygen consumption observed in response to FCCP has been attributed to the increased rate of oxidative phosphorylation in the mitochondria. In response to FCCP glucose consumption transiently decreases and then remains at a decreased level.

In the presence of FCCP, K^+, although still able to depolarize the plasma membrane, is no longer able to affect the mitochondria. Figure 3-7 shows the effect of increasing K^+ at an islet in the presence of FCCP on glucose consumption. The large transient decrease in glucose consumption observed in the absence of FCCP does not occur in the presence of FCCP. This suggests that the direct effect of depolarizing plasma membrane potential and increasing $[Ca^{2+}]_i$ is not responsible for the transient change in glucose consumption during a K^+ pulse.

Conclusions

Oscillations in $[Ca^{2+}]_i$, oxygen and glucose level occur in response to a glucose challenge. The presence of extracellular Ca^{2+} is required for the appearance of oscillations in oxygen and glucose consumption. Furthermore, when $[Ca^{2+}]_i$ is kept constant no metabolic oscillations occur and disrupting the mitochondrial membrane potential disrupted metabolic oscillations. Increasing $[Ca^{2+}]_i$ independently of metabolic

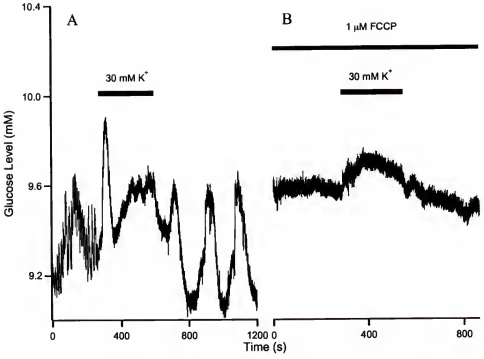

Figure 3-7 Effect of pulsing K^+ on glucose level in the presence of 1 μm FCCP. (A) Pulsing extra-islet K^+ levels reveals a transient increase in glucose level. (B) At the same islet pulsing extra-islet K^+ in the presence of 1 μM FCCP does not cause a transient increase in glucose level.

factors forces an increase in oxygen consumption and a decrease in glucose consumption. This is paralleled during normal metabolic oscillations as shown by simultaneous measurements of $[Ca^{2+}]_i$, glucose and oxygen consumption [Jun00]. Which indicated that at an islet glucose levels oscillate in phase with $[Ca^{2+}]_i$, and oxygen levels oscillate out of phase with $[Ca^{2+}]_i$ [Jun00]. Thus, it can be concluded that changes in $[Ca^{2+}]_i$ are required for changes in oxygen and glucose levels to occur. However, in the absence of glycolysis spontaneous oscillations in $[Ca^{2+}]_i$ do not occur; therefore, the contribution of glucose metabolism in oscillation generation cannot be ignored.

CHAPTER 4
GLUCOSE TRANSPORT INTO ISLETS OF LANGERHANS

Introduction

In response to a glucose challenge beta cells, contained in pancreatic islets of Langerhans, secrete insulin. There is a generally accepted consensus model describing glucose induced insulin secretion (GSIS) in beta-cells [Dee00, Hen00, Kom97, Mat96, New95]. Glucose enters the beta-cell via glucose transporters and is metabolized to produce increased ATP:ADP ratio. The increase in ATP:ADP ratio closes K_{ATP} channels, depolarizing the cell membrane [Ash84, Coo84, Koh98]. Cell depolarization triggers voltage gated Ca^{2+} channels, increasing intracellular Ca^{2+} concentration ($[Ca^{2+}]_i$) [Ror88]. The increase in $[Ca^{2+}]_i$ triggers insulin secretion.

Two glucose transporters have been identified in beta-cells. About 80% of glucose is transported into the beta-cell via Glut2 transporters; Glut1 transports the remaining glucose [Yas92]. Glut2 is an reversible transporter, allowing glucose to be transported into and out of the cell, resulting in an equilibrium between glucose levels on either side of the membrane [Hel71]. To insure a linear increase in beta-cell response during a glucose challenge Glut2 has a high K_m for glucose (17-20 mM) [Gou97]. Glut1 can only transport glucose into the beta-cell and has a much lower K_m (1.6 mM) than Glut2. Thus, Glut1 allows transport glucose into the beta-cell during fasting blood glucose levels, preventing cell starvation. The two transporters work together to insure healthy beta-cells capable of rapid response during a glucose challenge.

Glucose metabolism has been linked to the regulation of Glut2 expression in beta cells [Che90, Fer93, Ina92, Pur93]. It has been reported that during hypoglycemic conditions *in vitro*, Glut2 expression is decreased in beta-cells, but not in liver [Che90]. Increasing glucose concentration, during islet incubation *in vivo* has resulted in upregulation in Glut2 expression [Ina92]. These data indicate that during times when an organism is under a constant glucose challenge the beta-cells are able adjust themselves to deal with the challenge.

A common experimental protocol involves changing buffer glucose concentrations while measuring intra-islet cellular activity, such as $[Ca^{2+}]_i$. Glucose enters the islets by diffusing through the extracellular spaces. This diffusion into the islet has often been assumed to take negligible time. However, the beta-cells at the periphery of the islet could be consuming the glucose immediately after the rise in glucose level; thus, the rise in glucose at the center of the islets would be much slower. We have utilized recently developed glucose sensors [Jun00] to investigate the glucose transport into islets. Monitoring the time taken for glucose levels at the center of an islet to reach a steady elevated state after an extra-islet change in glucose levels enabled glucose transport into the islets to be investigated. Utilizing mannoheptulose, an inhibitor of GK we investigated the effect of glucose consumption on equilibration time. Incubation of islets in varying glucose concentrations revealed the effect of Glut2 and GK expression on glucose transport into the islet. Lastly, the effect of decreasing extracellular Ca^{2+} levels were also monitored.

Experimental

Islet Isolation and Culture

Islets of Langerhans were isolated from mice pancreata using ductal injection of collagenase buffer (1 mg/mL) as described previously [Hua95]. Islets were plated on nunc plates for microsensor experiments and incubated 2-4 days in RPMI 1640, containing 2, 11, or 22 mM glucose, supplemented with 10% fetal bovine serum and 1% penicillin-streptomycin and placed in an incubator at 37°C humidified in 95% air and 5% CO_2.

Oxygen and Glucose Microsensor Fabrication and Measurements in Single Islets

Oxygen and glucose sensors were prepared as described previously [Jun99a, Jun99b, Jun00]. The oxygen microsensors are composed of 25 μm diameter platinum wire, with etched tips (3-9 μm), recessed into a glass pipette, sealed with epoxy and coated with cellulose acetate. Glucose sensors are similar to the oxygen sensors but before coating with cellulose acetate, platinum is plated into the recess and glucose oxidase is immobilized in the platinum matrix.

Plates containing islets were placed on a Zeiss Axiovert 35 microscope and perfused with modified Krebs-Ringer buffer (KRB) buffer containing 20 mM HEPES, 118 mM NaCl, 5.4 mM KCl, 2.4 mM Ca^{2+}, 1.2 mM $MgSO_4$, 1.2 mM KH_2PO_4, and 5 mM $NaHCO_3$ at 37°C. Using an insert the volume of the plates was reduced to 200 μL and under perfusion it took 24.8 s to completely change the buffer content. Oxygen was continuously flowed over the plates for glucose measurements. Microsensors were held at –0.6 V or 0.6 V, for oxygen and glucose respectively, versus Ag/AgCl reference electrode and inserted into the islet using Burleigh piezoelectric drivers (PCS-250).

Amperometric data were filtered at 20 Hz and acquired at 100 Hz using a digidata board from Axon Instruments and an IBM compatible personal computer.

Chemicals and Reagents

Platinum wire was obtained from Johnson Matthey, silver epoxy from Epoxy Technology, Inc., and epoxy from Miller-Stephenson Chemical Company. Reagents for culture media were acquired from Life Technologies, Inc. All other chemicals were obtained from Fisher or Sigma.

Results and Discussion

Glucose transport into islets was investigated using glucose sensors placed 70 μm towards the center of the islet. The time taken for glucose level inside the islet to change from 10% to 90% was monitored. The sensors were always implanted to a depth of 70 μm towards the center of the islet. Figure 4-1A shows the temporal resolution of the perfusion system. It took 20 +/- 1 s (n=8) for 10 to 90% change in glucose concentration. Comparing Figure 4-1A and B indicates that the time required for glucose levels to equilibrate inside an islet is much slower than the response time of the perfusion system. Islets with diameters of 160-180 μm required 160 +/- 13 s (n=6) for equilibration of intra-islet glucose levels. Oscillations in glucose consumption were observed at the islets in the presence of 10 mM glucose.

Islet Size

Islet shape can be approximated as a sphere, and glucose transport into an islet occurs in three dimensions; thus, transport of glucose into an islet will be dependent on islet size. Figure 4-2A compares glucose transport into islets of different size. Although

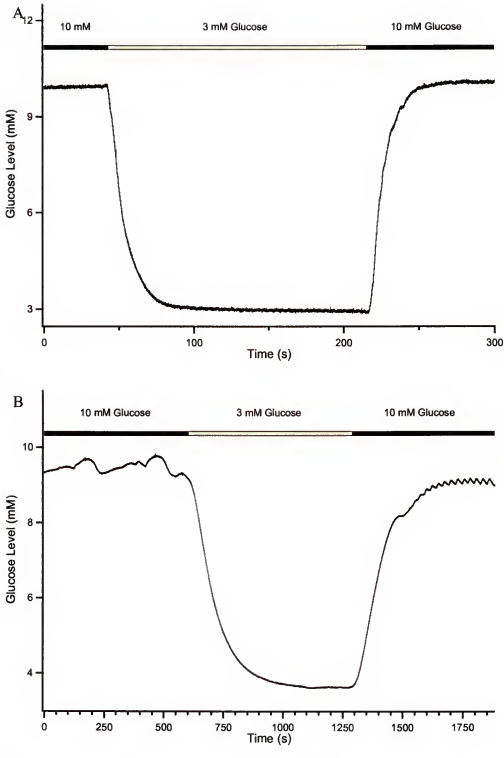

Figure 4-1 Glucose measurements at islets utilizing glucose sensors. (A) Response time of the perfusion system during a change of glucose concentration between 3 and 10 mM, as measured by glucose sensor in the absence of an islet. (B) Recording made at a glucose sensor implanted in the center of a 220 μm islet during a change in extra-islet glucose concentration from 3 to 10 mM.

the sensors were implanted to the same depth into each islet, the glucose equilibration time was much slower at larger islets (Fig 4-2B). Islets with diameters of 150-165 μm had t_R = 100 +/- 3 s (n=6), whereas islets with diameters of 180-220 μm had t_R = 177 +/-7 s (n=3). Since, glucose diffusion into islets occurs in three dimensions, the time lag in glucose equilibration is due to the longer path glucose has to move along the horizontal plane in larger islets.

Glucokinase Inhibition

Inhibition of glucose metabolism utilizing mannoheptulose, a competitive inhibitor of glucokinase [Coo64, Swe96], resulted in decreased t_R (Fig4-3). The t_R for islets in the presence of mannoheptulose was 122 +/- 11 s (n=3) versus 180 +/- 11 (n=6) for control islets (160-200 μm diameter). This suggests that the long time to reach steady state glucose levels within an islet after a change in extra-islet glucose level is partially due to the consumption of glucose by peripheral beta-cells in the islet.

Glucose Incubation Concentration

Table 4-1 shows the effect of incubating islets in different concentrations of glucose on glucose transport. Increasing the incubation glucose level to 22 mM increased the amount of time required for glucose to enter and leave the islet by an average of 160% versus islets incubated at 11 mM glucose. Comparing islets incubated for 2-3 days in different glucose levels, as in Figure 4-4, shows that islets incubated at higher glucose levels exhibit a delay in t_R. These data show that glucose diffusion into islets is delayed by changes occurring in the islets in response to glucose incubation concentration.

Previous studies have observed a change in the amount of Glut2 expressed in islets in response to changing glucose incubations concentrations [Che90, Fer93, Ina92,

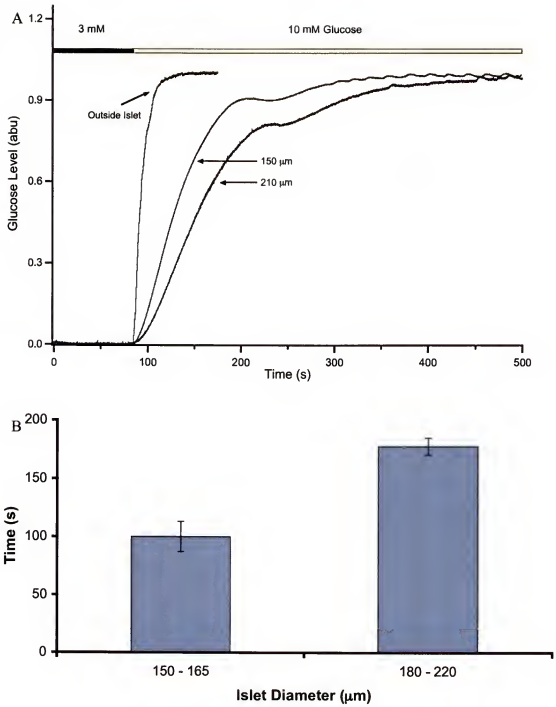

Figure 4-2 Effect of islet diameter on glucose equilibration in an islet. (A) With sensors implanted 70 µm into an islet the time taken for glucose level to equilibrate in response to changing extra-islet glucose levels from 3 to 10 mM increased with increasing islet diameter. The current traces were converted to 0 to 1 scale for easy visual comparison of plots. (B) Comparing t_R for glucose equilibration at islets for diameter ranges of 150-165 µm (n=6) and 180-220 µm (n=7). ($p<0.001$)

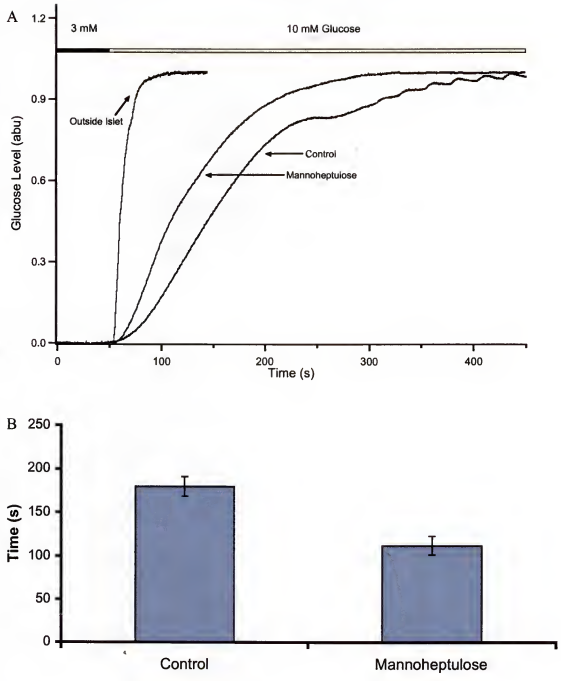

Figure 4-3 Effect of inhibiting glucokinase on glucose transport. (A) Current traces were converted to 0 to 1 scale with the start of glucose level increase superimposed for ease of comparison. Islets incubated in 10 mM mannoheptulose and 11 mM glucose prior to experiments, control islets were incubated in only 11 mM glucose. Glucose levels were monitored utilizing sensors implanted 70 μm into islets with diameters of 160-220 μm during a glucose change from 3 to 10 mM. (B) t_R of glucose equilibration, following a glucose change from 3 to 10 mM in islets exposed to 10 mM mannoheptulose (n=3) versus control (n=6) islets. ($P<0.005$)

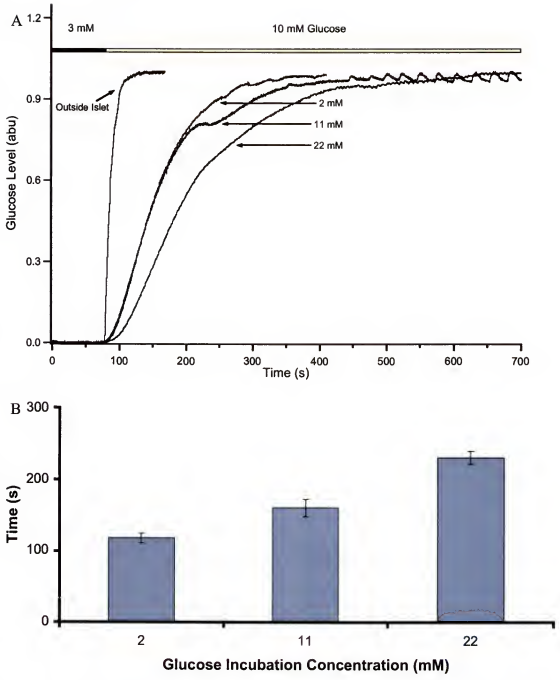

Figure 4-4 Effect of glucose incubation concentration on glucose transport into islets. (A) Current traces converted to 0 to 1 scale with start of glucose level increase superimposed for ease of comparison. Islets (160-180 μm diameter) were incubated in 2, 11 or 22 mM glucose for 2-3 days. Sensors were implanted 70 mm into the islet and glucose levels were monitored during an extra-islet glucose change between 3 and 10 mM. (B) Comparison of t_R for glucose equilibration in islets incubated in 2 (n=6), 11 (n=6) and 22 (n=8) mM glucose. ($p<0.01$ for 2 versus 11 mM glucose, $p<0.0005$ for 22 versus either 2 or 11 mM glucose)

Pur93]. The decrease in Glut2 expression observed in islets incubated at low glucose concentrations [Ina92] could explain the decrease in t_R observed in islets incubated at 2 mM glucose. A decrease in Glut2 transporters would decrease the amount of glucose transported into peripheral beta-cells during glucose diffusion into the islet; thus, decreasing the amount of time required for glucose equilibration within islets. However, the levels of other enzymes relevant for glucose transport and utilization by beta-cells may also be affected during incubation in different glucose levels.

Table 4-1 Effect of incubating islets in different levels of glucose on time required for glucose concentration at center of islet to change after extracellular glucose concentration was changed. Islets were incubated in 2, 11, or 22 mM glucose for 2-3 days.

Extracellular glucose change	Glucose incubation concentration		
	2 mM	11 mM	22 mM[a]
3 to 10 mM	122 +/- 14 s	142 +/- 19 s	215 +/- 10 s
10 to 3 mM	131 +/- 5 s	138 +/- 25 s	235 +/- 14 s
Average	126 +/- 7 s	140 +/- 14s	225 +/- 9 s

a Time taken for glucose transport into islets incubated with 22 mM glucose were significantly different from all other islets (99% confidence).

Extracellular Ca^{2+}

Decreasing the extracellular Ca^{2+} at an islet decreases the glucose consumption at islets (Chapter 3). Thus, the amount of glucose consumed by peripheral beta-cells in the islet would decrease in the absence of extracellular Ca^{2+}, decreasing the amount of time for glucose transport into the center of the islet. Table 4-2 shows the effect of lowering extracellular Ca^{2+} on glucose transport at an islet. Removal of extracellular Ca^{2+} increased the time required for glucose equilibration into the islet by 153 % during a change in extracellular glucose level from 3 to 10 mM. This shows that in the absence of

Ca^{2+} not only is oxygen consumption decreased (as discussed in Chapter 3), but also the equilibration of glucose into the islets is decreased. This may be the result of a direct action of Ca^{2+} on Glut2 transporters in beta-cells; however, a mechanism for this has not been previously reported. It is interesting to note that changing extra-islet Ca^{2+} levels had no effect on the equilibration time required after a glucose change from 10 to 3 mM. In no other set of experiments did the t_R of glucose equilibration act differently for the 3 to 10 mM glucose switch versus the 10 to 3 mM glucose switch.

Table 4-2 Effect of extracellular Ca^{2+} on time required for glucose level in at the center of an islet to change after switching glucose concentration from 3 to 10 or 10 to 3 mM glucose. Islets were incubated in 11 mM glucose for 3 days.

Extracellular glucose change	2.45 mM Ca^{2+}	0.1 mM Ca^{2+}
3 to 10 mM	77 +/- 8 s[a]	118 +/- 14 s[a]
10 to 3 mM	108 +/- 7 s	106 +/- 11 s

a Time taken for glucose transport into islet after changing extracellular glucose from 3 to 10 mM in the presence of 2.45 versus 0.1. mM Ca^{2+} is significantly different (90% confidence).

Conclusions

Equilibration of glucose level in islets is dependent on many factors. Glucose enters the islets through extracellular spaces within the islet. Decreasing glucose utilization by peripheral beta-cells and decreasing glucose incubation concentration decreases the amount of time required for glucose equilibration to occur within an islet. Glucose equilibration in an islet is not instantaneous; therefore, interpretation of results obtained at islets during experiments utilizing a step change in buffer glucose level need to take the time of glucose transport into islets into account.

CHAPTER 5
OTHER METABOLIC FACTORS

Introduction

To maintain glucose homeostasis, beta-cells, contained in islets of Langerhans, secrete insulin in response to a glucose challenge. Type 2 diabetics are characterized by the inability to secrete sufficient amount of insulin to maintain glucose homeostasis. Insulin secretion in healthy individuals is pulsatile [Goo77, Lan79]; however, this pulsatility is lost in type 2 diabetics [Mat83, Ora88]. In single islets insulin secretion is pulsatile in single islets during a glucose challenge [Bar96, Ber93, Ber94, Gil93], which is paralleled by oscillations in intracellular Ca^{2+} concentration ($[Ca^{2+}]_i$) [Gil93], glucose and oxygen consumption [Jun00].

The consensus model of glucose stimulated insulin secretion (GSIS) describes the mechanism of insulin secretion. Glucose enters the beta-cell through Glut2 transporters and is metabolized through glycolysis producing increased levels of ATP, NADH and pyruvate. Pyruvate enters the mitochondria and is metabolized through the citric acid cycle. The reducing equivalents from NADH enter the mitochondria through either the malate-aspartate shuttle or the glycerol-3-phosphate shuttle. NADH and the products from the citric acid cycle enter oxidative phosphorylation, further increasing the ATP:ADP ratio [Duk94, Eto99a, Eto99b, Sch97]. The increase in ATP:ADP ratio closes ATP sensitive K^+ (K_{ATP}) channels depolarizing the cell. Cell depolarization opens voltage gated Ca^{2+} channels, which increases $[Ca^{2+}]_i$. The increase in $[Ca^{2+}]_i$ stimulates insulin secretion through an unknown mechanism.

Investigations into beta-cell function often utilize Krebs Ringer Buffer (KRB), which contains biological levels of salts but no amino acids. However, there is concern that in the absence of amino acids, beta-cells will not function properly [Muk95]. Some studies have shown that application of amino acids change glucose induced oscillations. In the presence of 0.1-0.5 mM glycine, sarcosine, alanine or arginine glucose induced oscillations in $[Ca^{2+}]_i$ were transformed into constant elevated state in 60% at single beta-cells [Ahm99, Mcc97, Ten92]. Additional studies found that the oxygen consumption rate at rat islets, βTC3 and βHC9 cells did not change in response to a glucose challenge in the presence of Dublecco's Modified Eagle Medium (DMEM), which is amino acid rich [Muk95, Pap98, Pap01]. Repeating the experiment in KRB resulted in a large increase in oxygen consumption rate; however, the oxygen consumption rate in DMEM was always higher than that in KRB [Muk95, Pap98, Pap01]. Insulin secretion rate in both DMEM and KRB showed increases in response to a glucose challenge [Muk95, Pap98, Pap01]; thus, the absence of response in oxygen consumption rate in DMEM was not due to inability of the cells to respond to a glucose challenge. It was suggested that the increase in oxygen consumption rate monitored in KRB resulted from nutrient starvation instead of upregulation of GSIS [Pap98]. To investigate the effect buffer utilized during experiments at single islets we monitored the change in oxygen level in islets in DMEM and KRB during a change in glucose concentration.

Type 2 diabetes is caused by the insufficient insulin secreted for activation of target tissue in response to a glucose challenge. The desensitization of insulin receptors at the target tissue has been the focus of many investigations into the cause of type 2 diabetes. Disruption of insulin receptor substrate 2 (IRS-2) resulted in type 2 diabetes in

mice [Wit98]. Variations in the gene encoding insulin receptor substrate - 1 (IRS-1) have been associated with development of type 2 diabetes in humans [Alm93, Ima94, Laa94]. Recently, with the observation that insulin stimulated insulin secretion (ISIS) occurs at beta-cells [Asp99b, Asp00], the focus of investigations into insulin receptors has expanded to include studies at beta-cells. It is possible that ISIS could affect cellular activity in the beta-cell through insulin receptors, by modulating the oscillations which occur. Variations in insulin receptors could in that case disrupt the oscillations observed at normal beta-cells. To investigate this possibility, we compared oxygen consumption at islets from IRS-1 knock-out and wild type murine islets.

In vivo Glut2 mRNA levels decrease in response to hypoglycemia (low blood glucose) and increase in response to hyperglycemia (high blood glucose) [Che90]. Isolated islets from fasted versus fed rats showed a decrease in insulin release in response to a glucose challenge [Zaw00]. The islets from fasted rats also showed a loss in first phase insulin secretion observed at islets from fed rats [Zaw00]. Monitoring Glut2 mRNA in isolated islets from normal fed animals showed higher mRNA concentrations when islets were incubated in higher glucose levels [Fer93, Ina92, Yas92]. This is indicative of higher expression of Glut2 in islets exposed high glucose levels for extended periods, which was supported by the observation of an increase in Glut2 protein monitored at islets during incubation in increased levels of glucose [Fer93]. In addition, as islet incubation glucose concentration increases, the K_m of Glut2 transporter and glucose utilization decrease, while the V_{max} of glucokinase (GK) and glucose utilization increase [Pur93]. To elucidate the effect of Glut2 expression and glucose utilization on

oscillations we monitored glucose levels at islets exposed to 10 mM glucose after incubation in 2, 11 or 22 mM glucose.

Experimental

Islet Isolation and Culture

Islets of Langerhans were isolated from mice pancreata using ductal injection of collagenase buffer (1 mg/mL) as described previously [Hua95]. Islets were plated on nunc plates for microsensor experiments and incubated 2-4 days in RPMI 1640, containing 11 mM glucose, supplemented with 10% fetal bovine serum and 1% penicillin-streptomycin and placed in an incubator at 37°C humidified in 95% air and 5% CO_2.

Oxygen and Glucose Microsensor Fabrication and Measurements in Single Islets

Oxygen and glucose sensors were prepared as described previously [Jun99a, Jun99b, Jun00]. Refer to Appendix A for detailed description of microsensor manufacture. The oxygen microsensors are composed of 25 μm diameter platinum wire, with etched tips (3-9 μm), recessed into a glass pipette, sealed with epoxy and coated with cellulose acetate. Glucose sensors are similar to the oxygen sensors but before coating with cellulose acetate, platinum is plated into the recess and glucose oxidase is immobilized in the platinum matrix.

For detailed description of islet isolation procedure and Amperometric setup refer to Appendices B and C. Plates containing islets were placed on a Zeiss Axiovert 35 microscope and perfused with modified Krebs-Ringer buffer (KRB) buffer containing 20 mM HEPES, 118 mM NaCl, 5.4 mM KCl, 2.4 mM Ca^{2+}, 1.2 mM $MgSO_4$, 1.2 mM KH_2PO_4, and 5 mM $NaHCO_3$ at 37°C. Using an insert the volume of the plates was

reduced to 200 μL and under perfusion it took 24.8 s to completely change the buffer content. Oxygen was continuously flowed over the plates for glucose measurements. Microsensors were held at –0.6 V or 0.6 V, for oxygen and glucose respectively, versus Ag/AgCl reference electrode and inserted into the islet using Burleigh piezoelectric drivers (PCS-250). Amperometric data were filtered at 20 Hz and acquired at 100 Hz using a digidata board from Axon Instruments and an IBM compatible personal computer.

Chemicals and Reagents

Platinum wire was obtained from Johnson Matthey, silver epoxy from Epoxy Technology, Inc., and epoxy from Miller-Stephenson Chemical Company. Reagents for culture media were acquired from Life Technologies, Inc. All other chemicals were obtained from Fisher or Sigma.

Results

Amino Acid Rich Media

A recent work has suggested that glucose cannot accelerate respiration in the presence of fuel rich media, such as Dublecco's Modified Eagle Medium (DMEM) [Pap98, Pap01]. To determine if glucose could still induce metabolic oscillations in such media, we examined the effect of glucose in DMEM on oxygen oscillations in islets. Figure 5-1 shows oscillations observed at islets in DMEM in the presence of 10 mM glucose, when glucose levels were decreased to 3 mM, oscillations ceased (data not shown). These results confirmed that glucose caused slow oscillations in oxygen level in response to 10 mM glucose in DMEM (Fig 5-1). Islets in the presence of DMEM and 10 mM glucose oscillated with a period of 285 +/- 23 s with a magnitude of 9.8 +/- 2.7 mmHg (n=4). However, the period of these oscillations should not be directly compared

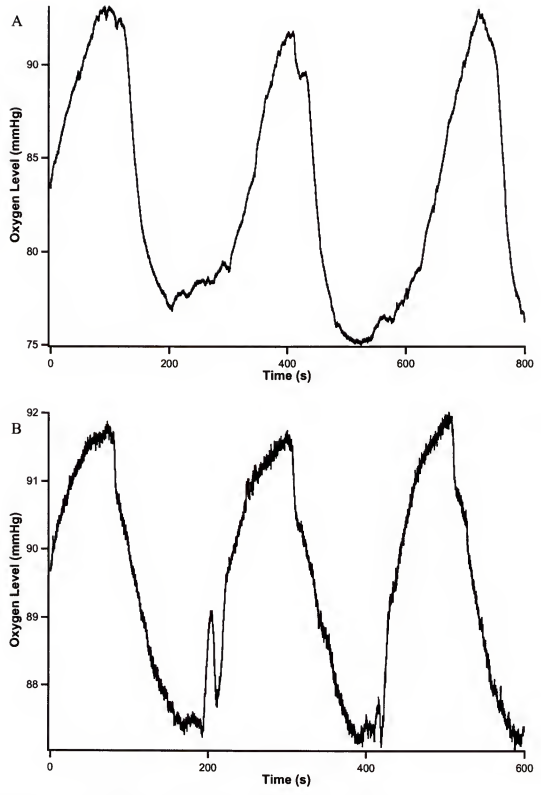

Figure 5-1 Oscillations in oxygen consumption observed at an islet in the presence of 10 mM glucose in either DMEM (A) or KRB (B).

to those observed with KRB, since extra-islet Ca^{2+} levels can modulate oscillation period, and DMEM and KRB contain 1.80 and 2.45 mM Ca^{2+}, respectively. Table 5-1 shows how the oxygen consumption in an islet increases in response to increased levels of glucose in DMEM. Oxygen levels, given as a percentage of oxygen level at 0 mM substrate, monitored in islets exposed to 10 mM glucose were 90.9 +/- 1.2 and 88.7 +/- 2.6% in DMEM and KRB, respectively. Thus, the change in oxygen level observed in response to a glucose challenge is not dependent on the amino acid content in the running buffer.

Our study was performed on islets incubated in RPMI for 3-5 days, whereas the previous study used freshly isolated islets. Previously it has been shown that $[Ca^{2+}]_i$ in islets in response to a 15 mM glucose challenge increased on day 4 to about 150% of that observed on day 1 [Gil94]. It is reasonable to believe that the increase in $[Ca^{2+}]_i$ in response to a glucose challenge after extended incubation in media would be paralleled by an increase in respiration. Thus the change in OCR in response to a glucose challenge in DMEM may be difficult to see due to the small change in oxygen consumption, which occurs immediately after isolation.

Table 5-1 Summary of oxygen levels at single islets exposed to different levels of glucose in DMEM.

Glucose Concentration (mM)	Oxygen Level (%)[a]
3	101 ± 2
10	91 ± 1
20	88 ± 4

a Oxygen level given as percentage of oxygen level at 0 mM substrate.

IRS-1 Knock-Out Islets

Table 5-2 summarizes the types of oscillations observed in oxygen level in response to 10 mM glucose at islets isolated from IRS-1 knock-out and wild mice. In the presence of 10 mM glucose, islets from wild type mice exhibited both fast and slow oscillations in oxygen consumption (Fig 5-2). However, islets from IRS-1 knock-out mice exhibited almost exclusively fast oscillations (Fig 5-2). IRS-1 affects the Ca^{2+} handling through SERCA as well as glycolytic enzymes. These data suggest that the signal coupling of IRS-1 activation may be involved in propagation of slow metabolic oscillations. However, other aspects of signal propagation required for the production of slow oscillations may have also been affected in this murine model.

Table 5-2 Summary of oxygen oscillations observed in response to 10 mM glucose at islets from IRS-1 knock-out and wild mice. Experiments were performed in KRB buffer with 2.45 mM Ca^{2+}. 11 islets from each type of mouse were monitored.

		IRS-1 K/O	Wild
Slow Oscillations	Period (s)	203 +/- 0	237 +/- 23
	Amplitude (mmHg)	1.8 +/- 0	3.3 +/- 0.5
	Number of islets displaying oscillations	1	5
Fast Oscillations	Period (s)	23 +/- 1	20 +/- 1
	Amplitude (mmHg)	0.8 +/- 0.1	0.9 +/- 0.1
	Number of islets displaying oscillations	10	6

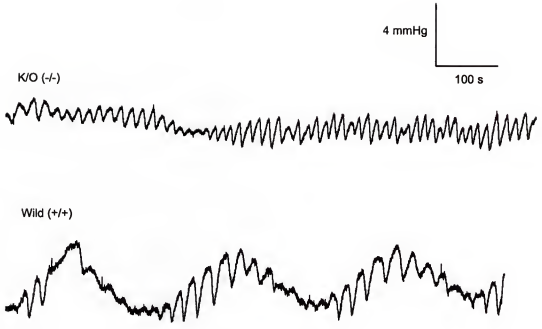

Figure 5-2 Oscillations in oxygen level observed at islets isolated from IRS-1 knock-out and wild mice in response to 10 mM glucose. An increase in oxygen level is equivalent to a decrease in oxygen consumption.

Glucose Incubation Concentration

Islets exhibit oscillations in glucose level when exposed to 10 mM glucose, comparing oscillation patterns for islets incubated in varying concentrations of glucose, as in Figure 5-3, indicates that glucose incubation concentration affect oscillation period and magnitude. The majority of islets (6 out of 7) incubated in 11 mM glucose exhibited slow, large amplitude oscillations; however, neither islets incubated in 2 nor 22 mM glucose exhibited as large a proportion of islets with slow oscillations (Table 5-3). Extrapolating these results to *in vivo* oscillations indicates that periods of hypoglycemia or hyperglycemia may further propagate symptoms in diabetics. This may also account

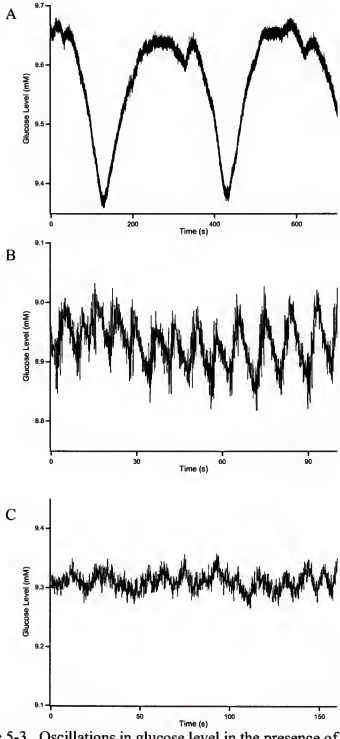

Figure 8. Figure 5-3. Oscillations in glucose level in the presence of 10 mM glucose at islets incubated in 2, 11, or 22 mM glucose. (A) 6 out of 7 islets incubated in 11 mM glucose displayed slow oscillations in glucose level, 232 +/- 19 s. (B) Islets incubated at 22 mM glucose showed slow oscillations of 164 +/- 36 s (n=2) or very fast oscillations 9 +/- 1 s (n=5). (C) 3 out of 6 islets incubated at 2 mM glucose showed low magnitude oscillations of medium period, 54 s (n=1), or fast period, 11 +/- 2 s (n=2). The other 3 islets displayed no discernable oscillations.

Table 5-3 Glucose induced oscillations in glucose levels in response to 10 mM glucose at islets incubated in 2, 11, or 22 mM glucose.

Glucose Incubation Concentration		2 mM	11 mM	22 mM
Slow Oscillations	Period (s)		232 ± 19	164 ± 36
	Amplitude (mM)		1.9 ± 0.4	1.90 ± 0.5
	Number of islets displaying oscillations[a]	0	6	2
Fast Oscillations	Period (s)	10.6 ± 1.8	44.0	9 ± 1
	Amplitude (mM)	0.07 ± 0.01	0.25	0.30 ± 0.06
	Number of islets displaying oscillations[a]	3	1	5
Fast Oscillations[b]	Period (s)		26 ± 3	7 ± 1
	Amplitude (mM)		0.7 ± 0.1	0.16 ± 0.02
	Number of islets displaying oscillations[a]	0	6	6

a Total number of islets monitored were 6, 7, and 7 for 2, 11, and 22 mM glucose incubation concentration, respectively.

b Fast oscillations observed after exposure of islets to 3 mM glucose. Islets incubated in 2 mM glucose did not display oscillations after exposure to 3 mM glucose.

for the resurgence of oscillations in insulin secretion seen in type 2 diabetics after a night of inhibiting insulin secretion and clamping blood glucose levels at 8 mM [Lae00].

Conclusions

Oxygen consumption monitored at islets in response to a glucose challenge, was similar in both KRB and DMEM. Thus, the presence of amino acids in the running buffer does not change the oxygen consumption monitored with our sensors at islets. However, in situations where experimental results are to be used for interpreting the behavior of an islet *in vitro*, it is recommended to perform *in vivo* experiments in an environment, which resembles conditions in vitro.

Islets from IRS-1 knock-out mice showed that slow oxygen oscillations at 10 mM glucose were absent in this murine model. This indicates that either the IRS-1 receptor is directly involved in metabolic oscillations or that other aspects of oscillation propagation are affected in this model.

Glucose incubation concentration affected oscillations observed in glucose levels at single islets. It was found that conditions, which resemble hypoglycemia or hyperglycemia, adversely affected the islets such that 10 mM glucose was no longer able to induce slow oscillations in glucose levels. Thus, maintaining good control over serum glucose levels in type 2 diabetics may improve pulsatility in serum insulin levels.

CHAPTER 6
INSULIN ELECTRODE

Introduction

Insulin is secreted by beta-cells, contained in pancreatic islets of Langerhans, in response to a glucose challenge. Type 2 diabetes results from the insufficient secretion of insulin for peripheral tissue activation. To investigate signal coupling required for normal insulin secretion, the ability to measure insulin secretion at single beta-cells is important.

Previously, secretory events from neurons have been monitored with good temporal resolution from single cells by amperometry as current spikes at microelectrodes [Wig91, Che94]. Exocytosis from beta-cells and neurons is similar, occurring as distinct secretory events from vesicles. Therefore, utilizing amperometry to monitor insulin secretion from beta-cells was investigated. Adapting a procedure for modifying electrode surfaces using ruthenium oxide and cyanoruthenate (Ru-O/CN-Ru) [Cox84] to microelectrodes, our group was able to detect insulin with limits of detection of 500 nM [Ken93]. These microelectrodes were successfully used to monitor insulin secretion from canine cells [Ken93, Hua95]. However, at biological pH (7.4) the modified electrodes degrade rapidly, making extended experiments impossible. Rodent beta-cells secrete lower quantities of insulin than human and canine beta-cells. When the modified microelectrodes were applied to murine beta-cells, they were found to be inadequate for reliable detection of insulin secretion. Another microelectrode utilized ruthenium-oxide-type catalytic film (RuOx) for insulin detection with detection limits of

23 nM. However, at physiological pH these electrodes were noisier, with the added difficulty of being sensitive to changes in glucose level [Gor97]. The RuOx microelectrode was the last reported microelectrode developed for direct detection of insulin.

To avoid modified microelectrodes, which degrade at biological pH, the possibility of utilizing unmodified electrodes was investigated. Previously, secretion of 5-hydroxytryptamine (5HT) from neurons had been monitored using bare carbon fiber microelectrodes [Mar97, Ter96]. Incubating beta-cells in media containing (5HT) results in the accumulation of 5HT in the insulin containing secretory vesicles. Monitoring the activity of 5HT loaded beta-cells with carbon fiber microelectrodes resulted in the observation of secretory spikes in response to various insulin secretagogues, such as glucose, tolbutamide, and K^+ [Asp97, Asp99a, Asp99b, Asp00, Bar96, Bar98, Bok00, Lak99, Par97, Par00, Rop02, Zho96]. By monitoring secretion with both modified and bare carbon fiber electrodes at 5HT loaded beta-cells, it was shown that 5HT is co-secreted with insulin [Asp97]. However, there are concerns that 5HT has detrimental effects on the ability of beta-cells to secrete insulin [Lin82, Zaw01].

Thus, a new microelectrode sensitive to insulin needs to be developed. To overcome the limitations of the previously described microelectrodes, developing a more stable modified microelectrode with high insulin sensitivity would aid research into insulin secretion. Modification of the Ru-O/CN-Ru plating procedure was investigated for increased stability and sensitivity of microelectrodes at biological pH. Initially the effects of varying the concentration of different components within the plating solution

were examined. Then the electrochemical plating procedure was investigated in hopes of increasing stability and sensitivity of the Ru-O/CN-Ru film.

The Ru-O/CN-Ru film is deposited on an electrode surface using an unreacted mixture containing $RuCl_3$ and $K_4Ru(CN)_6$ using potential cycling. The resulting film is believed to contain a mixture of $Ru(CN)_6^{3-,4-}$ and $Ru^{3+,2+}$, although the exact conformation of the film is unknown [Cox84]. It was observed that organic disulfides, such as cysteine, were oxidized at the electrode surface, due to the three disulfide bonds present in insulin, the electrode was tested for insulin sensitivity [Cox89].

Experimental

Chemicals and Reagents

Epoxy resin was obtained from Miller-Stephenson Chemical Company. All other chemicals were obtained from Fisher or Sigma.

Electrode Manufacture and Testing

Bare carbon fiber microelectrodes were manufactured as previously described [Asp97, Hua95]. Briefly, a carbon fiber filament, 9 μm diameter, was inserted into a glass capillary (1.2 mm O.D. × 0.68 mm I.D. × 4") and pulled into two electrodes. Tips of the electrodes were cut to yield a 12 μm opening which was sealed with epoxy resin (3 g hot Epon 828 containing 0.5 g *m*-phenylenediamine hardener). The epoxy was allowed to cure overnight. The electrodes were baked at 100 and 150 °C for 2 hours each to harden the epoxy. Electrodes were stored at room temperature until use. Prior to modification of the electrode surface, the electrodes were polished at an angle of 30°, cleaned using isopropyl alcohol and sonicated in de-ionized water. The electrodes were

backfilled with mercury and a silver wire was placed in the electrode to provide an electrical connection.

Ru-O/CN-Ru electrodes were prepared as previously described [Ken93]. Bare carbon fiber microelectrodes polished at an angle of 30° were placed in a solution of N_2-purged 2 mM $RuCl_3$, 2 mM $K_4Ru(CN)_6$ and 0.5 M KCl, pH 2.0, counter a calomel reference electrode, and the potential was cycled using an EI400 bipotentiostat, between 0.46 and 1.06 V for 25 minutes. Modifications of the Ru-O/CN-Ru plating procedure included varying concentrations of $RuCl_3$ and $K_4Ru(CN)_6$ components of the plating solution. Electrochemical plating method was also varied. Cyclic voltammograms were taken during the to plating process to observe development of the Ru-O/CN-Ru film.

Electrodes were tested in either phosphate or bicarbonate buffer. Phosphate buffer contained 10 mM $NaH_2PO_4 \cdot H_2O$, 12 mM $Na_2HPO_4 \cdot 7H_2O$ and 120 mM NaCl, pH 7.4. Bicarbonate buffer contained 118 mM NaCl, 5.4 mM KCl, 2.4 mM $CaCl_2$, 1.2 mM $MgSO_4$, 3 mM glucose, and 24 mM $NaHCO_3$. Prior to experiments, bicarbonate buffer was bubbled with 5% CO_2 for 20 minutes to establish a pH of 7.4. A stock solution of 1 mM insulin was prepared in 16 mM HCl and could be kept in the freezer for up to 3 days. Calibration solutions for electrode testing were made as dilutions of the insulin stock solution. Samples utilized as blanks were prepared identically to the insulin calibration solutions (including use of 16 mM HCl stock solution), without the addition of insulin.

A perfusion system utilizing a flow cell was used to test the electrodes. Buffer solution was pumped (Harvard Apparatus syringe pump model 11) into a six-port valve, which allowed pneumatic switching between buffer and sample solution, into a test cell. The test cell contained an inlet, 2 mm in diameter, into which the electrode was

positioned with a micromanipulator. Insulin was detected at the modified electrodes at 0.85 V using an EI400 bipotentiostat, with a calomel reference electrode. Each experiment lasted approximately 2 minutes. Between experiments the electrodes were "rested" for 5 minutes at a potential of 0.4 V to reduce degradation of the Ru-O/CN-Ru film.

Results and Discussion

Figure 6-1A shows the voltammogram observed at the end of the electrochemical plating of Ru-O/CN-Ru using the original plating procedure [Cox84], hereafter designated as procedure A.

Components of Plating Solution

The effect of $RuCl_3$ concentration in the plating solution was evaluated. Increasing the concentration of $RuCl_3$ from 2.0 to 2.3 mM showed an increase in peak to peak current monitored during plating of Ru-O/CN-Ru. Comparing voltammograms in Figure 6-1A and B shows the increased change in anodic versus cathodic current in response to increasing $RuCl_3$ concentration from 2.0 to 2.3 mM, keeping in mind that the total plating time for volatmmogram B was only 40 minutes as compared to 2 hours for A. However, only a slight increase in signal was observed (Table 6-1). Further increases in the $RuCl_3$ concentration to 4.0 mM showed no increases in peak to peak current observed during plating procedure or current observed in response to 10 μM insulin.

Previously, the KCl solution was always N_2-purged prior to plating. However, it was found that N_2-purging of the KCl solution was detrimental to the plating procedure. Cyclic voltammograms are similar for microelectrodes manufactured in N_2-purged and air equilibrated KCl solutions (Figure 6-1A and 6-2B). However, it was observed that

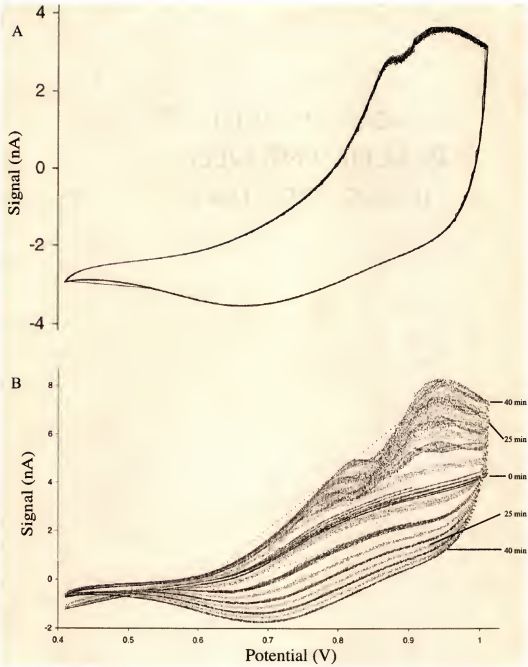

Figure 6-1 Cyclic voltammograms taken during electrochemical modifications of microelectrodes with Ru-O/CN-Ru. (A) Voltammogram observed at the end of 2 hours of the electrochemical plating of Ru-O/CN-Ru using deposition procedure A. (B) Voltammograms taken every 5 minutes during 40 minutes of cycling potential from 0.46 to 1.06 V during electrochemical plating. Plating solution contained 2.3 mM $RuCl_3$ and 2.0 mM $K_4Ru(CN)_6$ in N_2-purged KCl solution.

Table 6-1 Effect of varying $RuCl_3$ component of plating solution during potential cycling for 40 minutes between 0.46 and 1.06 V. KCl solution was N_2 purged prior to use. Signal monitored during 3rd injection of insulin during testing.

Concentration of $RuCl_3$ in plating solution	n	Peak to peak current[a] (nA)	Signal in response to 10 μM insulin (pA)
2.0	5	6.2 +/- 0.5	3.5 +/- 0.3
2.3	4	8 +/- 1	4.5 +/- 0.2
4.1	4	8 +/- 2	---

a Peak anodic versus peak cathodic current measured during potential cycling.

plating with N_2-purged KCl solution resulted in electrodes, which exhibited much faster degradation of signal. The signal recorded from electrodes manufactured utilizing procedure A in response to 10 μM insulin, degraded to below 3 pA before the 5th injection of sample during electrode testing. At electrodes manufactured in air equilibrated KCl solution a signal of 3 pA in response to 10 μM insulin could be monitored during the 5th and often the 6th sample injection during the testing phase.

During further investigation into the plating of Ru-O/CN-Ru onto the surface of microelectrodes, 2.3 mM $RuCl_3$ and 2 mM $K_4Ru(CN)_6$ was utilized in air equilibrated KCl solution.

Electrochemical Plating Procedure

Changing the electrochemical plating procedure was investigated to observe its effect on the stability and sensitivity of the Ru-O/CN-Ru layer. Holding the potential constant at 1.06 V for 15 minutes, without cycling the potential during the plating process, resulted in microelectrodes, with improved insulin sensitivity (Table 6-2). These microelectrodes also showed improved stability versus microelectrodes plated utilizing cycling potential. The plating procedure utilizing only cyclic potential showed signal degradation to below 3 pA in response to 10 μM insulin, prior to the 5th sample injection

during testing phase, the electrodes plated with constant potential displayed currents could be tested to an average of 14 injections during testing phase (n=4).

Table 6-2 Effect of changing electrochemical plating procedure microelectrode stability and signal.

Plating Procedure	Peak anodic versus peak cathodic signal during electrochemical plating (pA)	Signal in response to 10 μM insulin taken during 3rd injection of insulin during testing (pA)	Number of runs before signal decreased below 3 pA in response to 10 μM insulin
15 min at 1.06 V	-------	8 +/- 3 n=6	14 n=6
5 min at 1.06 V 25 min cycling at 0.46 to 1.06 V	11 +/- 2 n=8	7.1 +/- 0.7 n=8	18 n=8
15 min at 1.06 V 25 min cycling at 1.06 to –0.24 V	9.5 +/- 0.5 n=5	3.8 +/- 0.2 n=4	6 n=4

Combining both a period of constant potential and potential cycling, resulted in improved electrochemical plating (Table 6-2). Figure 6-2B shows the first and last cyclic voltammogram of a microelectrode plated using a constant potential for 5 minutes at 1.06 V followed by 25 minutes of potential cycling between 0.46 and 1.06 V (referred to as procedure B). Comparing Figure 6-2A and B shows that the first cyclic voltammogram observed (darker colored plot) during plating is much further developed after holding the potential constant for 5 minutes at 1.06 V than electrodes which are plated using only potential cycling. The electrodes made using procedure B for Ru-O/CN-Ru plating displayed improved stability and signal as compared to all previous procedures tested.

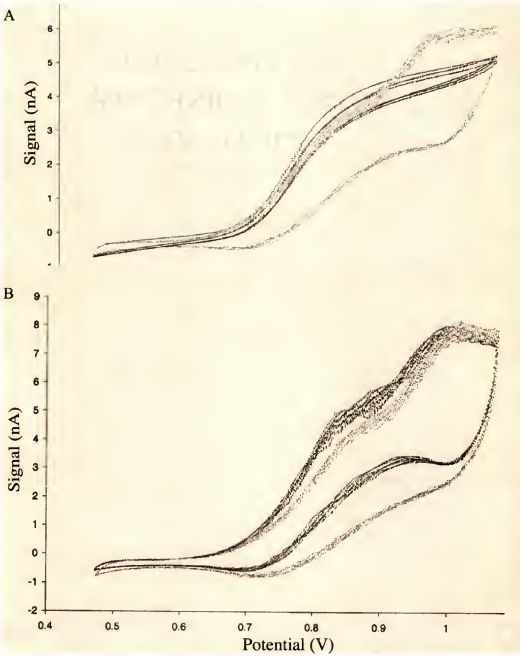

Figure 6-3 Initial and final voltammograms taken during electrochemical plating of Ru-O/CN-Ru film using 2.3 mM $RuCl_3$ and 2.0 mM $K_4Ru(CN)_6$ in air equilibrated KCl solution. (A) Initial and final voltammograms taken during potential cycling between 0.46 and 1.06 V. (B) Initial and final cyclic voltammograms taken during potential cycling between 0.46 and 1.06 V, following 5 minutes of constant potential at 1.06 V.

The signal of these electrodes would initially drop drastically during testing; however, after 14 minutes (by the 3rd injection of sample during testing) the signal would stabilize with relatively high sensitivity. Testing the electrodes for 2 minutes, with 5 minutes rest at 0.4 V between runs, resulted in stable signal for close to 2 hours (18 injections); however, only 36 minutes were spent at the working potential.

Another modification of the electrochemical plating procedure investigated the effect of increasing the voltage range used for potential cycling. Figure 6-3A shows the voltammogram observed during cycling of the potential from 0.46 V to – 0.24 V during electrochemical plating. These microelectrodes did not exhibit improved signal or stability. Combining a constant potential held at 1.06 V for 15 minutes prior to cycling the potential between –0.24 and 1.06 V was also attempted. Figure 6-3B shows the cyclic voltammograms taken during the first and last potential cycling during the plating procedure. As noted in Figure 6-2B, another microelectrode plated with constant potential prior to cycling the potential, the voltammogram of the first potential cycle is much more developed than that seen in the absence of plating with constant potential. The electrodes plated with an initial potential of 1.06 V followed by 25 minutes of cycling potential between –0.24 and 1.06 V did not exhibit improved stability or sensitivity as compared to microelectrodes plated using procedure B (Table 6-2).

Plating electrodes in 2.3 mM $RuCl_3$ and 2.0 mM $K_4Ru(CN)_6$ in air equilibrated KCl solution produced the most stable Ru-O/CN-Ru film. Electrochemical plating using a combination of 5 minutes at 1.06 V followed by 25 minutes of potential cycling between 0.46 and 1.06 V resulted in the most successful plating of microelectrodes

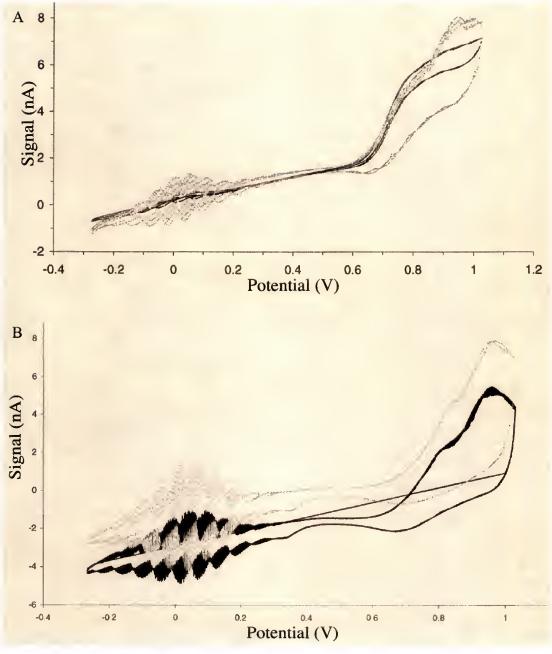

Figure 6-3 Cyclic voltammograms of electrochemical modification utilizing potential cycling between –0.24 and 1.06 V. Plating solution contained 2.3 mM $RuCl_3$ and 2.0 mM $K_4Ru(CN)_6$ in air equilibrated KCl solution at a pH of 2.0. (A) Initial and final voltammograms during 25 minutes of Ru-O/CN-Ru plating using only potential cycling. (B) Initial and final voltammograms during 25 minutes of potential cycling after 15 minutes of constant potential at 1.06 V.

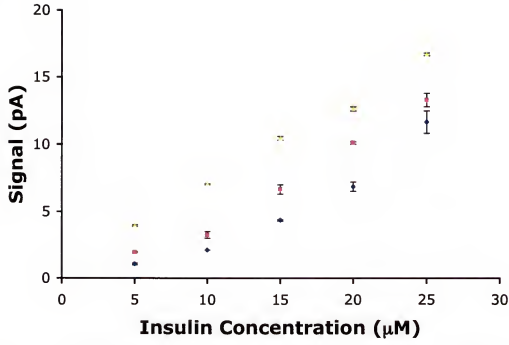

Figure 6-4 Calibration of three insulin sensitive electrodes modified 5 minutes at a constant potential of 1.06 V, followed by 25 minutes of potential cycling from 0.46 to 1.06 V. Each point represents three different runs.

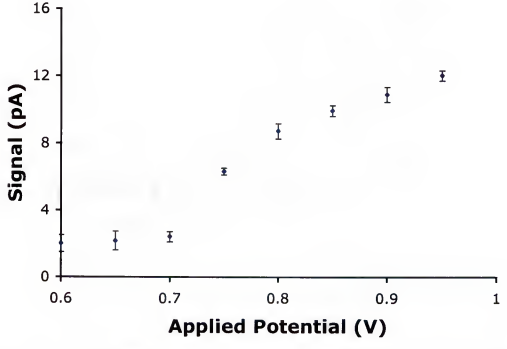

Figure 6-5 Hydrodynamic voltammogram using 10 mM insulin at a microelectrode modified using 5 minutes at constant potential of 1.06 V, followed by 25 minutes of potential cycling from 0.46 to 1.06 V.

(procedure B). Figure 6-4 shows a calibration plot for three different insulin electrodes modified as described using procedure B. Each electrode had a slightly different limit of detection but all had linear responses to insulin. A hydrodynamic voltammogram (Figure 6-5) was performed on this type of electrode showing that the working potential cancan be dropped to 0.75 V without a significant loss of signal, although, the lower working potential will greatly increased stability of the electrode surface.

Conclusions

The modification of the Ru-O/CN-Ru plating process resulted in microelectrodes with increased stability and sensitivity as compared to the original plating process. Plating carbon fiber microelectrodes at 1.06 V for 15 minutes and then cycling the potential from 0.46 to 1.06 V for 15 minutes in plating solution containing 2.3 mM $RuCl_3$ and 2 mM $K_4Ru(CN)_6$ in air equilibrated KCl solution produced in the most stable and sensitive electrodes. However, these microelectrodes were not sensitive enough for insulin detection at single mouse beta cells.

Investigating the use of platinum electrodes for Ru-O/CN-Ru plating may result in more sensitive insulin electrodes. Utilizing microelectrodes with a recessed tip filled with a porous layer of conducting material, such as the platinum plated in electrodes utilizing enzymatic solutions [Jun00], could improve the amount of Ru-O/CN-Ru film deposited onto the electrode surface due to the increase in surface area afforded by the porous layer of the electrode. The porous layer of conducting material would also act to entrap the Ru-O/CN-Ru. With the dual role of the porous layer for increased surface area and entrapment of Ru-O/CN-Ru, stability and sensitivity of the modified electrodes could be improved. Recently a new ruthenium metallodendrimer electrode was designed for insulin detection, which is stable at pH 7.0 [Che01]. This electrode is a glassy carbon

electrode, which is too big to measure insulin secretion from single cells, but modifying the procedure for a carbon fiber electrode could produce an electrode capable of monitoring insulin secretion from single beta-cells.

CHAPTER 7
SUMMARY AND FUTURE DIRECTIONS

Summary

Insulin secretion, $[Ca^{2+}]_i$, glucose and oxygen levels have been shown to oscillate during separate measurements at islets of Langerhans. During multiple sets of simultaneous measurements of two of these analytes, it has been shown they all oscillate in parallel. Utilizing glucose and oxygen sensors developed in our laboratory the chemical mechanism behind these oscillations has been investigated. It was discovered that slow oscillations in metabolism require the presence of stimulatory levels of glucose, or sub-stimulatory levels of glucose in the presence of GA. These data indicate that slow oscillations in islets were driven by glycolysis, with either glucokinase or phosphofructokinase as the main driving force. Fast oscillations in oxygen consumption can be observed in the presence of glyceraldehyde, but neither pyruvate nor methyl pyruvate was able to initiate fast oscillations. However, alpha-ketoisocaproate was able to induce fast oscillations in oxygen consumption after incubation of the islet with fura-2. Thus, it is likely that changes in $[Ca^{2+}]_i$ are driving fast oscillations in the absence of glycolytic substrates, such as glyceraldehyde.

In the absence of extracellular Ca^{2+}, no oscillations in metabolism were observed. Changes induced in $[Ca^{2+}]_i$ through control of K_{ATP} channels caused changes in both oxygen and glucose consumption. However, no spontaneous oscillations were observed in the absence of metabolic substrates; thus, it is unlikely that Ca^{2+} is the main source of oscillations.

Islets from IRS-1 knock-out mice showed that slow oxygen oscillations at 10 mM glucose were absent in this murine model. IRS-1 affects the Ca^{2+} handling through SERCA as well as glycolytic enzymes. Thus, the signal coupling of IRS-1 activation may be involved in propagation of slow metabolic oscillations; however, it must be kept in mind that other aspects of oscillation propagation may also be affected in this model.

Increasing glucose incubation concentration increases Glut2 expression and glucose utilization. It was demonstrated that glucose incubation concentration affects the presence of fast and slow oscillations monitored at islets in the presence of 10 mM glucose. Thus, Glut2 and glucose utilization are important factors in oscillation generation.

We have shown that oscillations in oxygen and glucose consumption occur in response to a glucose challenge. Only glucose was able to induce slow oscillations in oxygen consumption and the removal of extracellular Ca^{2+} prevented oscillations. Thus, slow oscillations are dependent on an interaction of glycolysis and $[Ca^{2+}]_i$. An absence of either factor will ablate metabolic oscillations. It was also shown that although only glucose could produce slow oscillations, glyceraldehyde could produce fast oscillations. Suggesting that slow and fast oscillations are controlled by different chemical mechanisms. The data presented suggest that fast oscillations are modulated by changes in Ca^{2+} and not modulated by metabolism.

Glucose enters islets by diffusion through extra-cellular spaces. After a change in extra-islet glucose level the equilibration of glucose into islets is relatively slow. Islet size, GK activity (as modulated by mannoheptulose), glucose incubation concentration, and the amount of extracellular Ca^{2+} present affect the time for glucose equilibration in

islets. Thus, glucose equilibration into islets is slowed down by glucose transport into peripheral beta-cells and glucose metabolism in these beta-cells.

Microelectrodes that can monitor insulin secretion from single beta-cells use a surface layer that catalyzes insulin oxidation. Modification of the plating procedure for Ru-O/Cn-Ru electrodes was attempted to improve the surface stability during measurements at biological samples. The final electrodes were more stable and sensitive than the original electrodes; however, these modified electrodes were still not capable of measuring insulin secretion from single murine beta-cells.

Future Directions

The incidence of type 2 diabetes is rising in North America; therefore, studying possible treatments for this group of diseases is vital. Insulin secretion oscillates in normal individuals; however, it is lost in type 2 diabetics. Therefore, continued research into the mechanism of oscillations is important.

Isolating the glycolytic enzyme(s) involved in creating the slow oscillations observed at islets in response to a glucose challenge is the first step in discovering the chemical mechanism behind oscillations. Designing plasma membrane permeable forms of glucose-6-phosphate (G6P), fructose-6-phosphate (F6P), and fructose-1,6-bisphosphate (F16bP) (the product of glucokinase, substrate of phosphofructokinase, and product of phosphofructokinase, respectively) is pertinent. Glucokinase and phosphofructokinase are the two main oscillatory enzymes in glycolysis between glucose and glyceraldehyde, which induce slow and fast oscillations, respectively. Monitoring oxygen consumption and $[Ca^{2+}]_i$ while applying G6P, F6P, and F16bP would elucidate which enzyme is responsible for slow oscillations. Expanding the studies of glycolytic fuels and the effects of $[Ca^{2+}]_i$ through monitoring insulin secretion simultaneously with

oxygen and glucose level, would give more insight into the cell signaling involved in insulin secretion.

Studies investigating the effect of $[Ca^{2+}]_i$ on oscillations in oxygen and glucose consumption should be continued, since we have only scratched the surface of this field. Investigating the effects of changing cAMP levels in an islet on oscillations of oxygen and glucose could yield insight into the mechanism of oscillations. Preliminary data show that increasing cAMP activity through the addition of forskolin, which has been shown to increase insulin secretion from single beta-cells [Boy89], changes the period and shape of oxygen oscillations observed at an islet (Fig. 7-1). cAMP may be either directly or indirectly involved in regulation of metabolism at beta-cells; thus, changing the oscillations observed at an islet.

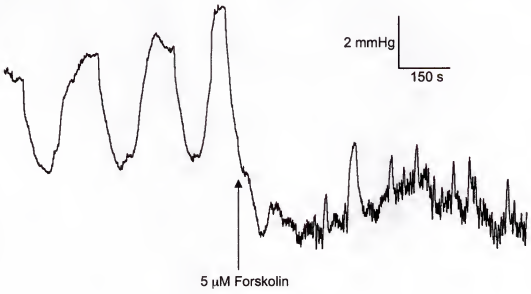

Figure 7-1 Effect of forskolin on 10 mM glucose induced oxygen oscillations at an islet.

The development of a fluorescent derivative for glucose, 2-[N-(7-nitrobenz-2-oxa-1,3-diazol-4-yl)amino]2-deoxy-D-glucose (2-NBDG), enabled glucose transport into beta-cells to be monitored [Yam00]. In our laboratory fluorescence methods are used to monitor $[Ca^{2+}]_i$ and insulin secretion (with Zn^{2+} as a marker ion). When coupling either of these two fluorescence measurements with an oxygen or glucose sensor, a large area of the beta-cell or islet is obscured by the physical presence of the sensor. Utilizing 2-NBDG as a tracer molecule for glucose, glucose uptake could be simultaneously monitored with insulin secretion or $[Ca^{2+}]_i$, without the interference of a microsensor.

Many diabetic organisms and genetically modified organisms area available for study. Monitoring oxygen and glucose consumption at islets of these organisms could elucidate errors in signal coupling that result in an increased risk of developing diabetes. Investigating these changes could aid research into the field of type 2 diabetes.

Knowledge of normal cellular activity and the effect of changing signaling pathways, as with knock out models, may eventually lead to therapies enabling control of glucose homeostasis in type 2 diabetics. It is believed that many cases of type 2 diabetes are un-diagnosed. Studies into cellular activity can lead to targets for screening genetic risk factors for type 2 diabetics. At risk individuals could then be identified and their blood glucose levels monitored from time to time allowing for early diagnosis of diabetes. Identifying genetic markers for diabetes may also allow for therapies to be applied to individuals before diabetes is reached.

APPENDIX A
OXYGEN AND GLUCOSE SENSORS

Chemicals and Reagents

27 gauge 1 1/2" needles were acquired from B-D (PrecisionGlide Needle #305136). 25 μm platinum wire and two part silver epoxy were from Alfa Aesar. Non-filamented, 1.2 mm O.D. × 0.69 mm I.D. × 10 cm long, borosilicate glass capillary was purchased from Carolina. Miller-Stphenson Chemical Co., Inc. provided Shell EPON resin 828 and metaphenylene diamine (MPDA). All other chemicals were purchased from Sigma-Aldrich or Fisher.

Sensor Manufacture

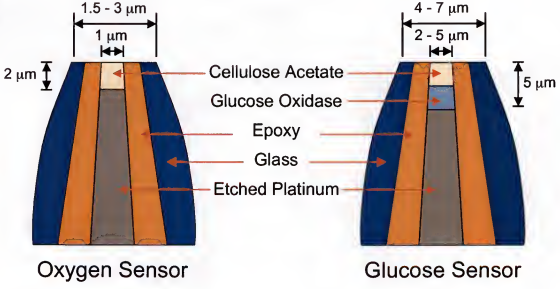

Figure A-1 Schematic of oxygen and glucose sensors showing approximate dimensions of sensor tips.

Glucose and oxygen sensors were prepared as previously described [Jun99a, Jun99b, Jun00]. A schematic of the sensor tips is shown in Figure A-1. 25 μm platinum

wire was placed into a 27 gauge, 1 1/2" needle and secured using two part silver epoxy. The needles were then baked for 1 hour at 100°C to cure the epoxy. The tip of the platinum wire was etched to a diameter of 1-4 μm by applying a 3.4 V – 2 ms square wave, counter a 1 mm platinum wire, was applied for 6-8 minutes in 3 mM KCN / 1 mM KOH aqueous solution. The wire was then rinsed in water and carefully placed in a pulled glass capillary. The tip of the glass capillary was cut so that the platinum wire could slightly protrude.

Hot epoxy was prepared in a disposable glass vial. 3 g EPON resin was slowly heated until a liquid viscosity resembling water was reached. Carefully the hardener, 0.5 g MPDA, was mixed into the hot resin. The tip of the capillary was dipped into the hot epoxy, to seal the platinum wire into the capillary. The epoxy was left to cure overnight and then baked at 100 °C for 2 hours and at 150 °C for 2 hours.

The capillary was backfilled with mercury and a silver wire was inserted for electrical connection. Using an aqueous 3 mM KCN solution and applying a 3.4 V – 2 ms square wave for about 1 minute the protruding platinum wire was etched resulting in the formation of a cavity in the tip of the electrode.

Oxygen sensors were dipped in 7% cellulose acetate in THF or acetone and left to dry overnight. The tip of glucose sensors were placed in saturated K_2PtCl_6 solution counter a SSCE reference electrode at -0.16 V for 3-4 minutes. Once the cavity at the tip of the glucose sensor was filled with platinum particles the tip of the sensor was submerged in 5% glucose oxidase solution for 10-15 minutes. After drying, the tip of the electrode was exposed to glutaric dialdehyde vapor for 1 – 2 minutes. Finally the glucose sensors were dipped in 7% cellulose acetate in THF and left to dry overnight.

Oxygen Sensors

During initial manufacture of oxygen sensors three point calibrations were utilized for sensor testing. Oxygen electrodes were placed in buffer solution, a potential of –0.6 V applied, and the buffer bubbled with O_2, air or N_2 from gas cylinders. The sensors, although each had a different signal, displayed linear calibration curves as shown in Figure A-2. Oxygen level in islets is below levels monitored in air equilibrated buffer; therefore, during experiments, the oxygen level at buffer equilibrated in air and N_2 was used for calibration. Only oxygen sensors displaying currents greater than 100 pA in air equilibrated buffer were utilized for islet experiments. Table A-1 summarizes the figures of merit for the oxygen sensors.

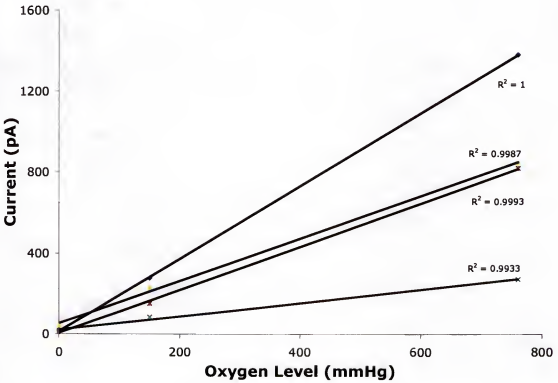

Figure A-2 Oxygen calibration curves for 4 different electrodes. Error bars were too small to see on this graph. At each point SEM < 2 pA.

Table A-1 Figures of merit for oxygen and glucose sensors.

	Oxygen Sensor	Glucose Sensor
Limit of Detection	< 3.0 mmHg	< 0.25 mM
Sensitivity	0.66 – 3.33 pA/mmHg	2.0 – 5.0 pA/mM
Peak to Peak Noise	0.05 – 0.2 pA	0.1 – 0.3 pA
Temporal Resolution	10 ms	100 ms

Glucose Sensor Calibration

During the initial design of glucose sensors, an oxygen dependence of the sensors was detected [Jun00]. Figure A-3 shows the effect of oxygen level on sensor calibration. With decreased oxygen level, the linear dynamic range of glucose sensors decreased.

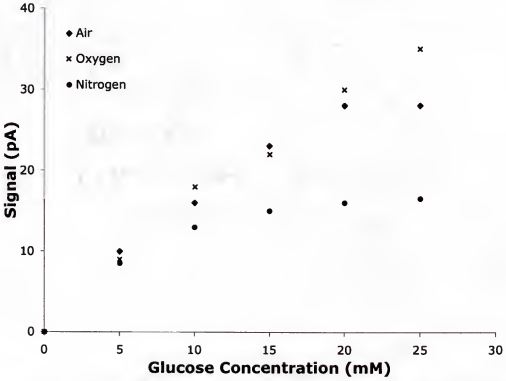

Figure A-4 Calibration curves for glucose sensor. Bubbling buffer in different oxygen levels resulted in a change of the linear dynamic range of sensors. Error bars are too small to discern on this plot, SEM < 0.2 pA.

Most experiments utilizing glucose sensors were performed with glucose levels between 3 and 10 mM glucose, the lowest level of oxygen required at the sensor was the equivalent of air equilibrated buffer. The oxygen level inside an islet is lower than outside the islet; thus, during glucose measurements, the buffer was bubbled with oxygen to increase the intra-islet oxygen level. For islet experiments only glucose sensors exhibiting currents above 2 pA/mM glucose were utilized.

APPENDIX B
MURINE ISLET ISOLATION

Mouse islets were isolated in house from CD-1 mice weighing 20-30 g. Islets from smaller mice tend to render smaller islets; therefore depending on the size of islets required mice of an appropriate size should be utilized. Usually only one mouse was used for islet isolation; however, if islets were dispersed into single cells, two mice were used for islet isolation. Buffers were prepared on day of dissection using 10X stock solutions of glucose (100 mM) and Ca^{2+} free 10X Hanks Balanced Salt Solution (HBSS), which were kept in the fridge for up to one month. 10X HBSS contained 1370 mM NaCl, 5.40 mM KCl, 0.410 mM NaH_2PO_4, and 100 mM HEPES, the pH was adjusted to 7.4 with NaOH. To prepare solutions for one mouse, on day of dissection 50 mL 10X HBSS, 25 mL 100 mM glucose and 1.0 mL 1 M $MgCl_2$ were poured into a 500 mL volumetric flask. Milli-Q water was used to fill the flask and pH was adjusted to 7.4 using NaOH. 50 mL of the solution (designated Mg^{2+}-HBSS) was filtered, using a sterile, 0.22 μm pore membrane filter into a 100 mL, autoclaved, glass flask. Using the same filter the remaining 450 mL HBSS was filtered into a 500 mL, autoclaved, glass flask, following the addition of 0.567 mL of 1 M $CaCl_2$ (designated Ca^{2+}-HBSS). Both of the solutions were kept on ice and bubbled with O_2 for 10 min. with an autoclaved gas dispersion stone. Immediately before dissection, 10-15 mL of 0.7 mM Collagenase Type XI was prepared with Mg^{2+}-HBSS. Only Collagenase with activities between 1200 and 1600 activity units were used to insure good islet yields and integrity.

Mice were sacrificed by cervical dislocation following anesthesia applied in a dessicator using metophane or halophane. 70% ethanol was utilized to disinfect the mice prior to dissection. A midline incision was made to expose the abdominal cavity and the intestines were moved out of the way using a cotton swab. The pancreatic duct was tied off between the liver and duodenum with silk suture cord to isolate it. The Collagenase solution was injected into the pancreas through the pancreatic duct utilizing a 27 gauge needle attached to a 5 mL syringe. At the point where the pancreatic duct attaches to the duodenum, a small, light colored, teardrop was located. Placing the duodenum on the tip of a finger the needle was inserted into the pancreatic duct at the point of the teardrop. In mice the pancreatic duct is very fragile so care had to be taken to not tear the duct. Slowly approximately 2.5 mL Collagenase solution was injected into the pancreatic duct, causing the pancreas to fill and distend. Starting at the spleen the pancreas was carefully removed and placed into an autoclaved, 20 mL siliconized scintillation vial. If the Collagenase injection was not successful the pancreas was still removed and chopped using dissecting scissors. 5 mL Collagenase solution was added to the vial, which was then placed in a 37° water bath for 12 minutes. During incubation with Collagenase the pancreatic tissue was digested, resulting in single islets and small pieces of acinar tissue. Following incubation 10 mL cold Mg^{2+}-HBSS was added to the vial, which was agitated briskly for 30 s. The contents of the vial were transferred into a sterile 50 mL centrifuge tube and the vial was rinsed with additional Mg^{2+}-HBSS, which was added to the centrifuge tube. The solution was allowed to settle for 4 minutes. 10-20 mL Ca^{2+}-HBSS was added to the tube and the solution in the vial was agitated using a sterile plastic transfer pipette. The tube was then left to settle, which allowed the denser islets to

separate from the acinar tissue. After 4 min. solution was aspirated from the top leaving the bottom 10 mL in the tube. The tube was filled with Ca^{2+}-HBSS solution and the contents of the tube agitated with a sterile plastic pipette. After 4 min. the solution was aspirated again. This was repeated 5-6 times to wash the majority of acinar tissue away.

After the last wash, the bottom 10 mL from the tube was transferred into two 60 mm culture dishes. The tube was then washed with 10 mL Ca^{2+}-HBSS, which was added to the culture dishes. Under a low magnification microscope the islets were identified by their dark brown color and uniform shape. The islets were hand picked using a 100 μL Eppendorf pipette with autoclaved pipette tips. Islets were placed into a 60 mm culture dish containing RPMI 1640 supplemented with 10% fetal bovine serum and 1% penicillin/streptomycin. Islets were then picked from the culture dish and placed in the center of 35 mm nunc culture dishes containing 3 mL supplemented RPMI 1640. The culture dishes were placed in an incubator at 37°C with 5% CO_2 and 95% air for 2-4 days.

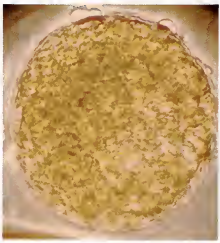

Figure B-1 Murine islets of Langerhans. (150 μm in diameter)

APPENDIX C
AMPEROMETRIC SETUP

A schematic of the Amperometric setup is depicted in Figure C-1. The cell chamber was positioned on an Axiovert inverted microscope. For perfusion experiments an insert was used with nunc culture dishes to reduce cell chamber volume to 200 μL. Buffer was introduced into the system using pressurized reservoirs. A five port valve enabled switching between four reservoirs. Prior to reaching the cell chamber the buffer was heated on-line using a Medical Systems Corporation temperature controller. Buffer was removed from the system through negative pressure. The system equilibrated to new buffer content in 21.1 +/- 0.6 s, n=8, as measured using glucose electrodes and switching between buffers with 3 and 10 mM glucose.

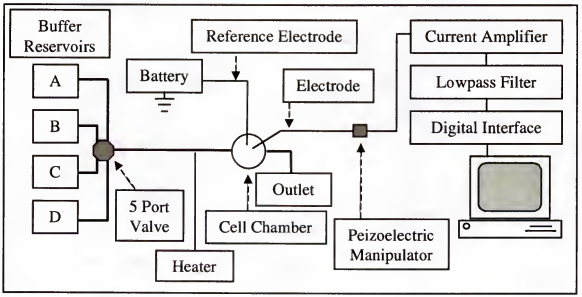

Figure C-1 Schematic of Amperometric setup. Cell chamber was placed on an Axiovert inverted microscope.

A potential was applied to the system using a battery connected to the reference electrode and to ground. The electrode was positioned in the cell chamber using micromanipulators. Fine adjustment of electrode position was accomplished using Burleigh piezoelectric micro-manipulators. A Keithley current amplifier was used to convert current from electrode into voltage. A Kron-Hite filter was used for low pass filtering of signal. The signal was acquired through an Axon DigiData digital interface and an IBM compatible personal computer, using Axopatch 8.0 acquisition program.

When glucose or oxygen levels were monitored in islets, the electrodes were inserted about 70 μm into the islet using the piezoelectric micro-manipulators, unless otherwise stated. Figure C-2 shows an electrode next to two islets. Care had to be taken to insure that the islets were positioned in the center of the culture dish otherwise the cell chamber insert would block access to the islet.

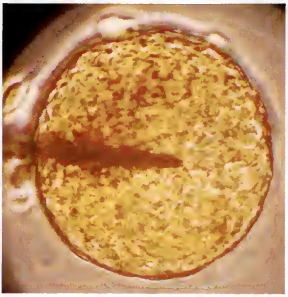

Figure C-2 Platinum electrode implanted into an islet of Langerhans (150 μm diameter).

LIST OF REFERENCES

Ahm99 Ahmed M, Grapengiesser E, Hellman B, *J Endocrin* 160, 191-195, **1999**.

Ain02 Ainscow EK, Rutter GA, *Diabetes* 51, S162-S170, **2002**.

Aiz00 Aizawa T, Kaneko T, Yajima H, Yamada S, Sato Y, Kanda Y, Kanda S, Noda M, Kadowaki T, Nagai M, Yamauchi K, Komatsu M, Hashizume K, *J Endocrinol* 166, 545-551, **2000**.

Alm93 Almind K, Bjorbaek C, Vestergaardt H, Hansen T, Echwald S, Pedersen O, *Lancet* 342, 828-832, **1993**.

And93 Andersen L, Dinsen B, Jorgensen PN, Poulsen F, Roder ME, *Clin Chem* 39, 578-582, **1993**.

Arm01 Armstrong DW, Zhang LK, He L, Gross ML, *Anal Chem* 73, 3679-3686, **2001**.

Ash73 Ashcroft SJH, Weerasinghe LCC, Randle PJ, *Biochem J* 132, 223-231, **1973**.

Ash84 Ashcroft FM, Harrison DE, Ashcroft SJH, *Nature* 312, 446-448, **1984**.

Asp97 Aspinwall CA, Brooks SA, Kennedy RT, Lakey JRT, *J Biol Chem* 272, 31308, **1997**.

Asp99a Aspinwall CA, Huang L, Lakey JRT, Kennedy RT, *Anal Chem* 71, 5551-5556, **1999**.

Asp99b Aspinwall CA, Lakey JRT, Kennedy RT, *J Biol Chem* 274, 6360-6365, **1999**.

Asp00 Aspinwall CA, Qian WJ, Roper MG, Kulkarni RN, Kahn CR, Kennedy RT, *J Biol Chem* 275, 22331-22338, **2000**.

Bal92 Balks HJ, Schmidt A, Prank K, Hemmer F, von zur Muhlen A, Brabant G, *J Clin Endocrinol Metab* 75, 1198-1203, **1992**.

Bar96 Barbosa RM, Silva AM, Tome AR, Stamford JA, Santos RM, Rosario LM, *Biochem Biophys Res Comm* 228, 100-104, **1996**.

Bar98 Barbosa RM, Silva AM, Tome AR, Stamford JA, Santos RM, Rosario LM, *J Physiol – London* 510, 135-143, **1998**.

Bed86 Bedoya FJ, Wilson JM, Ghosh AK, Finegold D, Matschinsky FM, *Diabetes* 35, 61-67, **1986**.

Bel71 Belmonte MM, Colle E, deBelle RC, Murthy DYN, *Union Med Can* 100, 778, **1971**.

Ber59 Berson SA, Yalow RS, *Nature* 184, 1648-1649, **1959.**

Ber93 Bergsten P, Hellman B, *Diabetes* 42, 670-674, **1993**.

Ber94 Bergsten P, Grapengeisser E, Gylfe E, Tengholm A, Hellman B, *J Biol Chem* 269, 8749-8753, **1994**.

Ble96 Bleich D, Chen SY, Bursten SL, Nadler JL, *Endocrin* 137, 4871-4877, **1996**.

Blu72 Blundell T, Dodson G, Hodkin D, Mercola D, *Adv Protein Chem* 26, 279-402, **1972**.

Bok00 Bokvist K, Holmqvist M, Gromada J, Rorsman P, *Pflug Arch Eur J Physiol* 439, 634-645, **2000**.

Boy89 Boyd AE, Rajan AS, Gaines KL, (Drasnin B, Melmed S, LeRoith D, Ed.), *Molecular and Cellular Biology of Diabetes Mellitus. Volume I: Insulin Secretion*, Alan R. Liss, Inc., New York, USA, 99, **1989**.

Bra98 Branstrom R, Efendic S, Berggren P-O, Larsson O, *J Biol Chem* 273, 14113-14118, **1998**.

But01 Butter NL, Hattersley AT, Clark PM, *Clin Chim Acta* 310, 141-150, **2001**.

Cao01 Cao Y, Smith WC, Bowsher RR, *J Pharm Biomed Anal* 26, 53-61, **2001**.

Che90 Chen L, Alam T, Johnson JH, Hughes S, Newgard CB, Unger RH, *Proc Natl Acad Sci* 87, 4088-4092, **1990**.

Che94 Chen TK, Luo G, Ewing AG, *Anal Chem* 66, 3031, **1994**.

Che01 Cheng L, Pacey GE, Cox JA, *Anal Chem* 73, 5607-10, **2001**.

Chi87 Childs GV, Unabia G, Burke JA, Marchetti C, *Am J Physiol* 252, E347-E356, **1987**.

Coo64 Coore HG, Randle PJ, *Biochem J* 91, 56-59, **1964**.

Coo84 Cook DL, Hales CN, *Nature* 311, 271-273, **1984**.

Cox84 Cox JA, Kulesza PJ, *Anal Chem* 56, 1021, **1984**.

Cox89 Cox JA, Gray TJ, *Anal Chem* 61, 2462-2464, **1989**.

Dee00 Deeney JT, Prentki M, Corkey BE, *Cell Develop Bio* 11, 267-275, **2000**.

Del02 Del Prato S, Marchetti P, Bonadonna C, *Diabetes* 51, S109-S116, **2002**.

Dem85 DeMoreno MR, Smith JF, Smith RV, *Anal Biochem* 151, 466-470, **1985**.

Den02 Deng B, Liu Z, Luo G, Ma H, Duan M, *J Pharm Biomed Anal* 27, 73-80, **2002**.

Duk94 Dukes ID, McIntyre MS, Mertz RJ, Philipson LH, Roe MW, Spencer B, Worley JF, *J Biol Chem* 269, 10979-10982, **1994**.

Emd80 Emdin SO, Dodson GG, Cutfield JM, Cutfield SM, *Diabetologia* 19, 174-189, **1980**.

Eng95 Engdahl JH, Veldhuis JD, Farrell PA, *J Appl Physiol* 79, 1977-1985, **1995**.

Epa85 Epanel RM, Stafford AR, Tyers M, Nieboer E, *Mol Pharmacol 27*, 366-374, **1985**.

Eto99a Eto K, Suga S, Wakui M, Tsubamoto Y, Terauchi Y, Taka J, Wizawa S, Noda M, Kimura S, Kasai H, Kadowaki T, *J Biol Chem* 274, 25386-25392, **1999**.

Eto99b Eto K, Tsubamoto Y, Terauchi Y, Sugiyama T, Kishimoto T, Takahashi N, Yamauchi N, Kubota N, Murayama S, Aizawa T, Akanuma Y, Aizawa S, Kasai H, Yazaki Y, Kadowaki T, *Science* 283, 981-985, **1999**.

Fer93 Ferrer J, Gomis R, Alvarez JF, Casamitjana R, Vilardell E, *Diabetes* 42, 1273-1280, **1993**.

Fra71 Frandsen EK, Grunnet N, *Eur J Biochem* 23, 588, **1971**.

Fro92 Froguel P, Vaxillaire M, Sun F, Velho G, Zouali H, Butel MO, Lesage S, Vionnet N, Clement K, Fougerousse F, Tanizaway Y, Weissenbach J, Beckmann JS, Lathrop GM, Passa P, Permutt MA, Cohen D, *Nature* 356, 162-164, **1992**.

Fro93 Froguel PH, Zouali H, Vionnet N, Velho G, Vaxillaire M, Sun F, Lesage S, Stoffel M, Takeda J, Passa PH, Permutt MA, Beckmann JS, Bell GI, Cohen D, *N Engl J Med* 328, 697-702, **1993**.

Gem93 Gembal M, Detimary P, Gilon P, Gao ZY, Henquin JC, *J Clin Invest* 91, 871-880, **1993**.

Gil92 Gilon P, Henquin JC, *J Biol Chem* 267, 20713-20720, **1992**.

Gil93 Gilon P, Shepherd RM, Henquin JC, *J Biol Chem* 268, 22265-22268, **1993**.

Gil94 Gilon P, Jonas JC, Henquin JC, *Diabetologia* 37, 1007-1014, **1994**.

Gil02 Gilon P, Ravier MA, Jonas JC, Henquin JC, *Diabetes* 51, S144-S151, **2002**.

Gol84 Gold G, Grodsky GM, *Experentia* 40, 1105-1114, **1984**.

Goo77 Goodner CJ, Walike BC, Koerker DJ, Ensinck JW, Brown AC, Chikeckel EW, Palmer J, Kalnasy L, *Science* 195, 177-179, **1977**.

Gor97 Gorski W, Aspinwall CA, Lakey JRT, Kennedy RT, *J Electroanal Chem* 425, 191-199, **1997**.

Gou97 Gould GW, *Facilitative Glucose Transporters*, R.G. Landes Company and Chapman & Hall, New York, U.S.A., **1997**.

Gun73 Gunnarsson R, Hellerstrom C, Horm Metab Res 5, 404-409, **1973**.

Hat92 Hattersley AT, Turner RC, Permutt MA, Patel P, Tanizaway Y, Chiu KC, O'Rahilly S, Watkins PJ, Wainscoat JS, *Lancet* 339, 1307-1310, **1992**.

Hed72 Hedeskov CJ, Hertz L, Nissen C, *Biochim Biophys Acta* 261, 388-397, **1972**.

Hel72 Hellman B, Sehlin J, Taljedal I, *Biochim Biophys Acta* 241, 147-154, **1971**.

Hel74 Hellman B, Idahl LA, Lernmark A, Sehlin J, Taljedal IB, *Arch Biochem Biophys* 162, 448-457, **1974**.

Hen90 Henquin JC, *Diabetes* 39, 1457-1460, **1990**.

Hen00 Henquin JC, *Diabetes* 49, 1751-1760, **2000**.

Hes71 Hess B, Boiteux A, *Annu Rev Biochem* 40, 237-258, **1971**.

Hir88 Hiriart M, Matteson DR, *J Gen Physiol* 91, 617-639, **1988**.

Hir95 Hiriart M, Sanchez-Soto MC, Ramirez-Medeles MC, Malaisse WJ, *Biochem Mol Med* 54, 133-137, **1995**.

Hol02 Hollingdal M, Juhl CB, Dall R, Sturis J, Veldhuis JD, Schmitz O, Porkensen N, *Diabetologia* 45, 49-55, **2002**.

Hua95 Huang L, Shen H, Atkinson MA, Kennedy RT, *Pro. Natl Acad Sci* 92, 9608, **1995**.

Hun96 Hunter SJ, Atkinson AB, Ennis CN, Sheridan B, Bell PM, *Diabetes* 45, 683-686, **1996**.

Hut80a Hutton JC, Malaisse WJ, *Diabetologia* 18, 395-405, **1980**.

Hut80b Hutton JC, Sener A, Herchuelz A, Atwater I, Kawazu S, Boschero AC, Somers G, Devis G, Malaisse WJ, *Endocrin* 106, 203-219, **1980**.

Hut82 Hutton JC, *Biochem J* 204, 171-178, **1982**.

Ima94 Imai Y, Fusco A, Suzuki Y, Lesniak MA, Dalfonso R, Sesti G, Bertoli A, Lauro R, Accili D, Taylor S, *J Clin Endocrin Metab* 79, 1655-1658, **1994**.

Ina92 Inagaki N, Yasuda K, Inoue G, Okamoto Y, Tano H, Someya Y, Ohmoto Y, Deguchi K, Imagawa KI, Imura H, Seino Y, *Diabetes* 41, 592-597, **1992**.

Ish00 Ishihara H, Wollheim CB, *IUBMB Life* 49, 391-395, **2000**.

Jij96 Jijakli H, Nadi AB, Cook L, Best L, Sener A, Malaisse WJ, *Arch Biochem Biophys* 335, 245-257, **1996**.

Job67 Jobsis FF, Duffield JC, *J Gen Physiol* 50, 1009-1047, **1967**.

Job68 Jobsis FF, Stainsgy WN, *Respir Physiol* 4, 292-300, **1968**.

Jon98 Jonas JC, Gilon P, Henquin JC, *Diabetes* 47, 1266-1273, **1998**.

Jun99a Jung SK, Aspinwall CA, Kennedy RT, *Biochem Biophys Res Comm* 259, 331-335, **1999**.

Jun99b Jung SK, Gorski W, Aspinwall CA, Kauri LM, Kennedy RT, *Anal Chem* 71, 3642-3649, **1999**.

Jun00 Jung SK, Kauri LM, Qian WJ, Kennedy RT, *J Biol Chem* 275, 6642-6650, **2000**.

Kan92 Kanatsuka A, Makino H, Yamaguchi T, Ohsawa H, Tokuyama Y, Saitoh T, Yamamura K, Miyazaki J, Yoshidas, *Diabetes* 41, 1409-1414, **1992**.

Ken93 Kennedy RT, Huang L, Atkinson MA, Dush P, *Anal Chem* 65, 1882, **1993**.

Ken02 Kennedy RT, Kauri LM, Dahlgren GM, Jung SK, *Diabetes* 51, S152-S161, **2002**.

Kje02 Kjems LL, Ravier MA, Jonas JC, Henquin JC, *Diabetes* 51, S177-S182, **2002**.

Koh98 Kohler M, Norgren S, Berggren PO, Fredholm BB, Larsson O, Rhodes CJ, Herbert TP, Luthman H, *FEBS Letters* 441, 97-107, **1998**.

Kom97 Komatsu M, Schermerhorn T, Noda M, Straub SG, Aizawa T, Sharp GW, *Diabetes* 46, 1928-1938, **1997**.

Koo96 Koopmans SJ, Sips HC, Krans HM, Radder JK, *Diabetologia* 39, 391-400, **1996**.

Kri00 Krippeit-Drews P, Dufer M, Drews G, *Biochem Biophys Res Comm* 267, 179-183, **2000**.

Kry85 Krystal G, Macdonald C, Munt B, Ashwell S, *Anal Biochem* 148, 451-460, **1995**.

Kry87 Krystal G, *Anal Biochem* 167, 86-96, **1987**.

Laa94 Laakso M, Malkki M, Kekalainen P, Kuusisto J, Deeb SS, *J Clin Invest* 94, 1141-1146, **1994**.

Lae00 Laedtke T, Kjems L, Porkensen N, Schmitz O, Veldhuis J, Kao PC, Butler PC, *Am J Physiol* 279, E520-E528, **2000**.

Lak99 Lakey JRT, Aspinwall CA, Cavanagh TJ, Kennedy RT, *Cell Transplant* 8, 691-698, **1999**.

Lan79 Lang DA, Matthews DR, Peto J, Turner RC, *N Engl J Med* 301, 1023-1027, **1979**.

Lan82 Lang DA, Matthews DR, Burnett M, Ward GM, Turner RC, *Diabetes* 31, 22-26, **1982**.

Lar96 Larsson O, Kindmark H, Branstrom R, Fredholm B, Berggren PO, *Proc Natl Acad Sci* 93, 5161-5165, **1996**.

Lem98 Lembert N, Idahl LA, *Diabetes* 47, 339-344, **1998**.

Lem01 Lembert N, Joos HC, Idhal LA, Ammon HPT, Wahl MA, *Biochem J* 354, 345-350, **2001**.

Len00 Lenzen S, Lerch M, Peckmann T, Markus T, *Biochim Biophys Acta* 1523, 65-72, **2000**.

Lia90 Liang Y, Najafi H, Matschinsky FM, *J Biol Chem* 265, 16863-16866, **1990**.

Lin82 Linstrom P, *Acta Biol Med Ger* 41, 1185-1190, **1982**.

Liu71 Liu BJ, Haist RE, Can J Physiol Pharmacol 49, 559-567, **1971**.

Liu01 Liu HJ, Strong RE, Krull IS, Cohen SA, *Anal Biochem* 298, 103-111, **2001**.

Lon91 Longo EA, Tornheim K, Deeney JT, Varnum BA, Tillotson D, Prentki M, Corkey BE, *J Biol Chem* 266, 9314-9319, **1991**.

Mac89 MacDonald MJ, *Arch Biochem Biophys* 270, 15-22, **1989**.

Mac97 MacDonald MJ, AlMasri H, JumelleLaclau M, Cruz MO, *Diabetes* 46, 1996-2001, **1997**.

Mag98 Magnus G, Keizer J, *Am J Physiol* 274, C1174-C1184, **1998**.

Mah99 Mahalingam B, Cuesta-Munoz A, Davis EA, Matschinsky FM, Harrison RW, Weber IT, *Diabetes*, 48, 1698-1705, **1999**.

Mal79 Malaisse WJ, Kawazu S, Herchuelz A, Hutton JC, Somers G, Devis G, Sener A, *Arch Biochem Biophys* 194, 49-62, **1979**.

Mar97 Marszalek PE, Farrell B, Verdugo P, Fernandez JM, *Biophys J* 73, 1169-1183, **1997**.

Mat83 Matthews DR, Naylor BA, Jones RG, Ward GM, Turner RC, *Diabetes* 32, 617-621, **1983**.

Mat90 Matschinsky FM, *Diabetes* 39, 647-652, **1990**.

Mat96 Matschinsky FM, *Diabetes* 45, 223-241, **1996**.

Mcc97 McClenaghan N, Berts A, Dryselius S, Grapengiesser E, Saha S, Hellman B, *Pancreas* 14, 65-70, **1997**.

Meg84 Meglasson MD, Matschinsky FM, *Am J Physiol* 246, E1-E13, **1984**.

Mer96 Mertz RJ, Worley JF III, Spencer B, Johnson JH, Dukes ID, *J Biol Chem* 271, 4838-4845, **1996**.

Mor81 Morrissey JH, *Anal Biochem* 117, 307-310, **1981**.

Muk95 Mukundan NE, Flanders C, Constantinidis I, Papas KK, Sambanis A, *Biochem Biophys Res Comm* 210, 113-118, **1995**.

New95 Newgard CB, McGarry JD, *Annu Rev Biochem* 64, 689-719, **1995**.

Nor97 Norman AW, Litwack G, *Hormones*, Academic Press, Orlando, USA, **1997**.

Ome93 O'Meara NM, Sturis J, Blackman JD, Roland DC, Polonsky KS, *Am J Physiol*, 264, E231-E238, **1993**.

Poa92 Opara EC, Hubbard VS, Burch WM, Akwari OE, *Endocrin* 130, 657-662, **1992**.

Ora88 O'Rahilly S, Turner RC, Matthews DR, *N Engl J Med* 318, 1225-1230, **1988**.

Orc77 Orci L, (Bajaj JS, Ed.) *Insulin and Metabolism*, Excerpta Medica, Amsterdam, Netherlands, 85-94, **1977**.

Orc85 Orci L, *Diabetologia* 28, 528-546, **1985**.

Orc88 Orci L, Vassalli JD, Perrelet A, *Sci Am* 259, 85-94, **1988**.

Ort00 Ortsater H, Liss P, Lund PE, Akerman KEO, Bergsten P, *Diabetologia* 43, 1313-1318, **2000**.

Pan74 Pantten U, Christians J, Kriegstein E, von Poser W, Hasselblatt A, *Diabetologia* 10, 149-154, **1974**.

Pao87 Paolisso G, Sgambato S, Passariello N, Scheen A, D'Onofrio F, Lefebvre PJ, *Diabetes* 36, 566-579, **1987**.

Pao88 Paolisso G, Sgambato S, Gentile S, Memoli P, Giugliano D, Varricchio M, D'Onofrio F, *J Clin Endocrin Metab* 67, 1005-1010, **1988**.

Pap98 Papas KK, Jarema MAC, Am. J. Physiol. 275, E1100-E1106, **1998**.

Pap01 Papas KK, Wu H, Colton CK, Weir GC, Hu S, *Diabetes* 50, A358, **2001**.

Par97 Paras CD, Kennedy RT, *Electroanal* 9, 203-208, **1997**.

Par00 Paras CD, Qian WJ, Lakey JR, Tan WH, Kennedy RT, *Cell Biochem Biophys* 33, 227-240, **2000**.

Pei92 Peiris AN, Stagner JI, Vogel RL, Nakagawa A, Samols E, *J Clin Endocrinol Metab* 75, 290-294, **1992**.

Per92 Permutt MA, Chiu KC, Tanizawa Y, *Diabetes* 41, 1367-1372, **1992**.

Por97 Porkensen N, Nyholm B, Veldhuis JD, Butler PC, Schmitz O, *Am J Physiol* 273, E908-E914, **1997**.

Por00 Porterfield DM, Corkey RF, Sanger RH, Tornheim T, Smith PJS, Corkey BE, *Diabetes* 49, 1511-1516, **2000**.

Pra90 Pralong WF, Bartley C, Wollheim CB, *Embo J* 9, 53-60, **1990**.

Pra94 Pralong WF, Spat A, Wollheim CB, *J Biol Chem* 269, 27310-27314, **1994**.

Pur93 Purrello F, Buscema M, Rabuazzo AM, Caltabiano V, Forte F, Vinci M, Vigneri R, *Diabetes* 42, 199-205, **1993**.

Qia00 Qian WJ, Aspinwall CA, Battiste MA, Kennedy RT, *Anal Chem* 72, 711-717, **2000**.

Rav99 Ravier MA, Gilon P, Henquin JC, *Diabetes* 48, 2374-2382, **1999**.

Ris97 Ristow M, Vorgerd M, Mohlig M, Schatz H, Pfeiffer A, *J Clin Invest* 100, 2833-2841, **1997**.

Ris99 Ristow M, Carlqvist H, Hebinck J, Vorgerd M, Krone W, Pfeiffer A, Muller-Wieland D, Ostenson CG, *Diabetes* 48, 1557-1561, **1999**.

Rol02 Roland JF, Henquin JC, Gilon P, *Diabetes* 51, 376-384, **2002**.

Rop02 Roper MG, Qian WJ, Zhang BB, Kulkarni RK, Kahn CR, Kennedy RT, *Diabetes* 51, 543-549, **2002**.

Ror88 Rorsman P, Ashcroft FM, Trube G, *Pfluger's Arch* 412, 597-603, **1988**.

Sch60 Schiebler TH, Schiessler S, *J Histochem Cytochem* 8, 312-313, **1960**.

Sch95 Schultz NM, Huang L, Kennedy RT, *Anal Chem* 67, 924-929, **1995**.

Sch97 Schuit F, DeVos A, Farfari S, Moens K, Pepeleers D, Brun T, Prentki M, *J Biol Chem* 272, 18572-18579, **1997**.

Sen78 Sener A, Kawazu S, Hutton JC, Boschero AC, Devis G, Somers G, Herchuelz A, Malaisse WJ, *Biochem J* 176, 217-232, **1978**.

She97 Shen H, Aspinwall CA, Kennedy RT, *J Chromatogr B Biomed Sci Appl* 689, 295-303, **1997**.

Shi01 Shiea J, Chang DY, Lin CH, Jiang SJ, *Anal Chem* 73, 4983-4987, **2001**.

Sil69 Sillero MAG, Sillero A, Sols A, *Eur J Biochem* 10, 345, **1969**.

Sta74 Starr JI, Rubenstein AH, (Jaffe BM, Behrman HR, Ed.), *Methods of Hormone Radioimmunoassay*, Academic Press, New York, **1974**.

Sto93 Storch MJ, Rossle M, Kerp L, *Dtsch Med Wochenschr* 118, 134-138, **1993**.

Swe96 Sweet IR, Li G, Najafi H, Berner D, Matschinsky FM, *Am J Physiol* 271, E606-E625, **1996**.

Tan54 Tanford C, Epstein J, *J Am Chem Soc* 76, 2170-2176, **1954**.

Tan00 Taniguchi S, Okinaka M, Tanigawa K, Miwa I, *J Biochem* 127, 289-295, **2000.**

Tao96 Tao L, Kennedy RT, *Anal Chem* 68, 3899-3905, **1996**.

Ten92 Tengholm A, McClenaghan N, Grapengiesser E, Gylfe E, Hellman B, *Biochimica Biophysica Acta* 1137, 243-247, **1992**.

Ter96 Terreni L, Gemma C, DeSimoni MG, *J Neurosci Met* 68, 71-79, **1996**.

Tor75 Tornheim K, Lowenstein JM, *J Biol Chem* 250, 6304-6314, **1975**.

Tor88 Tornheim K, *J Biol Chem* 263, 2619-2624, **1988**.

Tor91 Tornheim K, Andres V, Schultz V, *J Biol Chem* 266, 15675-15678, **1991**.

Tor97 Tornheim K, *Diabetes* 46, 1375-1380, **1997**.

Tru81 Trus MD, Zawalick WS, Burch PT, Berner DK, Weill VA, Matschinsky FM, *Diabetes* 30, 911-922, **1981**.

Vel97 Velho G, Blanche H, Vaxillaire M, BellanneChantelot C, Pardini VC, Timsit J, Passa P, Deschamps I, Robert JJ, Weber IT, Marotta D, Pilkis SJ, Lipkind GM, Bell GI, Froguel P, *Diabetologia*, 40, 217-224, **1997**.

Wes96 Westerlund J, Hellman B, Bergsten P, *J Clin Invest* 97, 1860-1867, **1996**.

Wes97 Westerlund J, Gylfe E, Bergsten P, *J Clin Invest* 100, 2547-2551, **1997**.

Wig91 Woghtman RM, Jankowski JA, Kennedy RT, Kawagoe KT, Schroeder TJ, Leszyszyn DJ, Near JA, Diliberto EJ, Viveros OH, *Proc Natl Acad Sci* 88, 10754, **1991**.

Wit98 Withers DJ, Gutierrez JS, Towery H, Burks DJ, Ren JM, Previs S, Zhang Y, Bernal D, Pons S, Shulman GI, Bonner-Weir S, White MF, *Nature* 391, 900-904, **1998**.

Yal60 Yalow RS, Berson SA, *J Clin Invest* 39, 1157-1175, **1960**.

Yam00 Yamada N, Nakata M, Horimoto N, Saito M, Matsuoka H, Inagaki N, *J Biol Chem* 275, 22278-22283, **2000**.

Yas92 Yasuda K, Yamada Y, Inagaki N, Yano H, Okamoto Y, Tsuji K, Fukumoto H, Imura H, Seino S, Seino Y, *Diabetes* 41, 76-81, **1992**.

Yos96 Yoshioka K, Oh KB, Saito M, Nemoto Y, Matsuoka H, *Appl Microbiol Biotechnol* 46, 400-404, **1996**.

Zaw97 Zawalich WS, Zawalich KC, *J Biol Chem* 272, 3527-3531, **1997**

Zaw00 Zawalich WS, Zawalich KC, *J Endocrin* 166, 111-120, **2000**.

Zaw01 Zawalich WS, Tesz GJ, Zawalick KC, *J Biol Chem* 276, 37120-37123, **2001**.

Zho96 Zhou Z, Misler S, *J Biol Chem* 271, 270-277, **1996**.

BIOGRAPHICAL SKETCH

Lisa Marie Kauri was born September 21, 1974, in Södra Sandby, Sweden. In 1983 she moved to Ottawa, Canada, with her family. She spent 5 years at the University of Ottawa earning a Bachelor of Science in biochemistry in 1995 and a Bachelor of Applied Science in chemical engineering in 1997. In May 1997 Lisa entered graduate school in the Chemistry Department at the University of Florida under the guidance of Dr Robert T. Kennedy. She completed her research in May 2002 obtaining a Doctor of Philosophy degree.

I certify that I have read this study and that in my opinion it conforms to acceptable standards of scholarly presentation and is fully adequate, in scope and quality, as a dissertation for the degree of Doctor of Philosophy.

Robert T. Kennedy, Chairman
Professor of Chemistry

I certify that I have read this study and that in my opinion it conforms to acceptable standards of scholarly presentation and is fully adequate, in scope and quality, as a dissertation for the degree of Doctor of Philosophy.

Weihong Tan
Associate Professor of Chemistry

I certify that I have read this study and that in my opinion it conforms to acceptable standards of scholarly presentation and is fully adequate, in scope and quality, as a dissertation for the degree of Doctor of Philosophy.

Nigel G.J. Richards
Associate Professor of Chemistry

I certify that I have read this study and that in my opinion it conforms to acceptable standards of scholarly presentation and is fully adequate, in scope and quality, as a dissertation for the degree of Doctor of Philosophy.

Jon D. Stewart
Assistant Professor of Chemistry

I certify that I have read this study and that in my opinion it conforms to acceptable standards of scholarly presentation and is fully adequate, in scope and quality, as a dissertation for the degree of Doctor of Philosophy.

Susan C. Frost

Susan C. Frost
Professor of Biochemistry and Molecular Biology

This dissertation was submitted to the Graduate Faculty of the Department of Chemistry in the College of Liberal Arts and Sciences and to the Graduate School and was accepted as partial fulfillment of the requirements for the degree of Doctor of Philosophy.

May 2002

Dean, Graduate School